https://doi.org/10.1016/j.quaint.2022.01.002

Quaternary International

Abrupt environmental changes during the last glacial cycle in Western Mediterranean (Formentera Island, Baleares, Spain)

--Manuscript Draft--

Manuscript Number:	QUATINT-D-21-00457
Article Type:	SI: PALEOCOASTS
Keywords:	Late Pleistocene; Climate; Balearic Islands; Sea level
Corresponding Author:	Teresa Bardaji Universidad de Alcalá Alcalá de Henares, Spain
First Author:	Teresa Bardaji
Order of Authors:	Teresa Bardaji
	Elvira Roquero
	Ana Cabero
	Caridad Zazo
	José L. Goy
	Cristino J. Dabrio
	María J. Machado
	Javier Lario
	Pablo G. Silva
	Antonio M. Martínez-Graña
Abstract:	A sedimentary sequence covering the entire last glacial cycle (period between Terminations I and II) outcrops along the south-eastern coast of Formentera Island. A detailed geomorphological, geological and sedimentological study, supported by geochemical, soil and soil-morphology analyses, magnetic susceptibility, phytolite content and luminescence dating (TL, OSL) allowed to reconstruct the environmental evolution of this coastal setting, and to frame it within the evolutionary pattern of the North Atlantic climate variability. Three highstands of sea level are identified in this island for MIS 5e, and a fourth one is attributed to MIS5a. MIS5 – MIS4 transition is characterized by soil development under a moist-warm climate and a descending sea level scenario. Aeolian units (72±7 ka BP) developed during MIS4 under prevailing northerly winds that persisted until the beginning of MIS3, when new aeolian dunes (54±5 ka BP) developed after a major sea-level lowstand. A sudden shift in prevailing winds occur within MIS3, when aeolian units (51±4 ka BP) grew under the influence of S-SW winds and moister climate, evidenced by a dense root bioturbation. The greater influence of northerly winds is attributed to the weakening of Atlantic Meridional Overturning Current (AMOC) in North Atlantic, and enhancement of westerlies in NW Euroe during colder periods. Periods of prevailing southerly winds and moister climate correlate well with warm Greenland Interstadials, and reinforcement of AMOC. Between 50 and 40ka, alluvial /colluvial sedimentary units punctuated by soil and calcrete development, witness the climatic variability recorded along this period in the North Atlantic. A sedimentary hiatus marks the first part MIS 2 with erosion and calcrete development characterizing the transit between MIS3 and MIS2. Above this erosional surface, a reddish alluvial sedimentary unit (20±2 ka BP – 17+2.4/-2.2) records the most humid and warm climate of the entire sequence (soil development, peak in magnetic susceptibility, phytolite content) that can be correlated with GS-2.1b, slightly warmer the other substadials of GS2.

Abrupt environmental changes during the last glacial cycle in Western Mediterranean (Formentera Island, Baleares, Spain)

T. Bardají[a,*], E. Roquero[b], A. Cabero[c], C. Zazo[d], J.L. Goy[e], C.J. Dabrio[f], M.J. Machado[g], J. Lario[h], P.G. Silva[i], A.M. Martínez-Graña[e]

[a] Universidad de Alcalá, Depto. Geología, Geografía y Medio Ambiente, 28871-Alcalá de Henares, Madrid, Spain
[b] Universidad Politécnica de Madrid, ETSI Agrónomos, Depto. Edafología, 28040-Madrid, Spain
[c] Escuela Politécnica Superior de Ecuador, Depto. Geología, 17-01-2759 Quito, Ecuador
[d] Museo Nacional de Ciencias Naturales, CSIC, Dpto. Geología, 28006-Madrid, Spain
[e] Universidad de Salamanca, Depto. Geología, 38008-Salamanca, Spain
[f] Universidad Complutense de Madrid, Depto. Estratigrafía, 28040-Madrid, Spain
[g] Universidad Nacional de Educación a Distancia, Av. Esparta s/n, 28232-Madrid, Spain
[h] Universidad de Salamanca, EPS Ávila, Depto. Geología, 05003-Ávila, Spain

* Corresponding author.
E-mail address: teresa.bardaji@uah.es (T. Bardají).

ABSTRACT

A sedimentary sequence covering the entire last glacial cycle (period between Terminations I and II) outcrops along the south-eastern coast of Formentera Island. A detailed geomorphological, geological and sedimentological study, supported by geochemical, soil and soil-morphology analyses, magnetic susceptibility, phytolite content and luminescence dating (TL, OSL) allowed to reconstruct the environmental evolution of this coastal setting, and to frame it within the evolutionary pattern of the North Atlantic climate variability. Three highstands of sea level are identified in this island for MIS 5e, and a fourth one is attributed to MIS5a. MIS5 – MIS4 transition is characterized by soil development under a moist-warm climate and a descending sea level scenario. Aeolian units (72±7 ka BP) developed during MIS4 under prevailing northerly winds that persisted until the beginning of MIS3, when new aeolian dunes (54±5 ka BP) developed after a major sea-level lowstand. A sudden shift in prevailing winds occur within MIS3, when aeolian units (51±4 ka BP) grew under the influence of S-SW winds and moister climate, evidenced by a dense root bioturbation. The greater influence of northerly winds is attributed to the weakening of Atlantic Meridional Overturning Current (AMOC) in North Atlantic, and enhancement of westerlies in NW Euroe during colder periods. Periods of prevailing southerly winds and moister climate correlate well with warm Greenland Interstadials, and reinforcement of AMOC. Between 50 and 40ka, alluvial /colluvial sedimentary units punctuated by soil and calcrete development, witness the climatic variability recorded along this period in the North Atlantic. A sedimentary hiatus marks the first part MIS 2 with erosion and calcrete development characterizing the transit between MIS3 and MIS2. Above this erosional surface, a reddish alluvial sedimentary unit (20±2 ka BP – 17+2.4/-2.2) records the most humid and warm climate of the entire sequence (soil development, peak in magnetic susceptibility, phytolite content) that can be correlated with GS-2.1b, slightly warmer the other substadials of GS2.

Keywords: Late Pleistocene; Climate; Balearic Islands; Sea level

1. INTRODUCTION

The last glacial cycle is defined as the period between Termination I and Termination II, period around which the last glacial stage took place diachronically around the globe (Hughes et al., 2013)., The climatic instability along this cycle in the North Atlantic region was dominated by large and abrupt climate shifts (e.g., Dansgaard et al., 1993; Rasmunsen et al., 2003; NGRIP Members, 2004; Bond et al. 1992; 1993; 1997; McManus al. 1999; Sarnthein et al., 2000; Zhang et al., 2017) shown in the detailed $\delta^{18}O$ and Ca^{2+} record from Greenland ice cores (Rasmussen et al., 2014). Up to 25 Greenland Stadials (GS) and 26 Interstadials (GI) as well as several of short-lived climatic oscillations of minor amplitude were defined in that record. GS and GI correlate well with the North Atlantic Dansgaard – Oescher events (D-O) during which climate alternated between full glacial and relatively mild conditions (Dansgaard et al., 1982). Heinrich events have been defined as cold spells characterized by the presence of ice rafted debris (IRD) in North Atlantic during this time span (Heinrich, 1988). They occur during stadials, but they do not last the entire stadial, so this term must be applied only if IRD are found in a particular record. In constrast, Heinrich Stadial (HS) refers to a stadial where a Heinrich event occurs (Rasmussen et al., 2014). Although not yet well understood (some possible causes summarised by Maslin et al. 2001), what these changes do attest to are the complex ocean-atmosphere connections encompassed by important changes in the Atlantic Meridional Overturning Circulation (AMOC), (McManus et al., 2004).

The Mediterranean basin holds a high sensitivity to global climatic changes due not only to its semi-enclosed nature (Martínez-Ruíz et al., 2015) but mainly to its latitudinal location between the colder/wetter Europe and warmer/dryer Africa land masses. In this sense, the Iberian Peninsula becomes a key area to evaluate (a) the teleconnections between the North-Atlantic and the Mediterranean Torner et al., 2019) and (b) the impact that past AMOC changes may have caused in western Mediterranean climatology, oceanography (e.g. Cacho et al., 1999; Hoogakker et al., 2004; Frigola et al. 2007, 2008; Moreno et al., 2007, 2010; Martrat et al. 2014) and vegetation (Sánchez-Goñi et al., 2005; 2020; Fletcher and Sánchez-Goñi, 2008). Data from the Iberian margin (Martrat et al., 2004) point to the occurrence of more frequent and of higher amplitude rapid climatic oscillations when compared with the three previous climate cycles.

The MIS5 - MIS1 interval has been widely studied in the southern and south-eastern coasts of the Iberian Peninsula as well as in Mallorca Island, and in a minor extent in Ibiza Island. Concerning sea level changes, Hearty (1987), Cuerda (1989), Hillaire-Marcel et al. (1996), Vessica et al. (2000), Zazo et al. (2003, 2008), Ginés et al. (2005, 2012), Tuccimei et al. (2006, 2012), Goy et al. (2006), Hearty et al. (2007) Bardají et al. (2009), Dorale et al. (2010), Onac et al. (2012) suggested millennial, suborbital-scale and, in some cases, centennial (Dabrio et al., 2011) changes.

The Balearic Islands are a key site to understand the climatic interactions between North Atlantic-Northern Europe and North Africa, and the coastal environmental response. These islands constitute the threshold between the colder waters of Gulf of Lions (Catalonian Provençal Basin) and the warmer Algerian Basin, forcing the Western Mediterranean oceanographic pattern (Fig. 1). Contrasting with the many studies on sedimentology, stratigraphy and chronology of Upper Pleistocene deposits carried out in the island of Mallorca (see a compilation in Ginés et al., 2012), research on these topics has been very scarce and almost non-existent for many years in Formentera Island (Balearic Islands). Among the scarce available information about the Late Pleistocene in Formentera, only a few references deal with marine deposits along the coasts of the island, especially those found at the southern foot of La Mola promontory (southeastern end of the island). These units contain the classic “Senegalese” warm fauna (*Strombus bubonius* or *Persististrombus latus, Conus testudinariu, Thais haemastoma*, etc) being thus assigned to the Last Interglacial, MIS 5 (Cuerda, 1989; Gàsser and Ferrer, 1997; Gásser, 1998). However, these marine deposits have not been included in the National Geological and Geomorphological Map where they are just referred as aeolian “white sands made of limestone grains and shell fragments” of Late Pleistocene age (Cabra et al., 2009).

Geomorphological and stratigraphic research on the transition from MIS5 to MIS1 in Formentera, allowed Goy et al. (2007) to select some of the most complete sedimentary sequences where this transition can be investigated in detail. Goy et al., (2010) reported the sea level changes recorded in Formentera along MIS 5e and the changing climatic history during the following glacial period, on the basis of sedimentary facies and morphosedimentary analyses, coupled with some optically stimulated luminescence (OSL) data. Bardají et al. (2013) recognized sea-level oscillations inside the second highstand of MIS 5e. Del Valle et al. (2020) proposed an environmental evolution of the island between MIS6 and MIS4/3, based on the sedimentary sequence outcropping at Cala en Baster supported by OSL data that constrained the MIS4-MIS5d time span. Finally, del Valle et al (2021) described an Upper Pleistocene sedimentary sequence along the southern cliffs of the island, analysing the interactions between coastal and terrestrial units. Analyses of last glacial terrestrial deposits in the area (Rose et al., 1999; González-Hernández et al., 2001; Clemmensen et al, 2001; Hodge et al., 2008; Fornós et al., 2008; Muhs et al., 2010; del Valle et al., 2018; 2020; 2021; Pomar et al., 2018) confirm the occurrence of important climate changes in the archipelago along this period.

We present here a multidisciplinary-multiproxy approach of the coastal response to the eustatic and climate changes occurred in Formentera Island between MIS5 and MIS1. The sedimentary succession outcropping along the southern cliff of the island, is continuous and complete enough to investigate the history of the eustatic and climatic evolution along the last glacial cycle, and to frame it within the evolutionary pattern of the North Atlantic. Geomorphological, sedimentological, pedological, palaeontological, magnetic susceptibility and geochemical studies have been applied in the reconstruction of the environmental evolution of these coastal systems. Chronology is approached by luminescence dating, and phytolith content has been determined for the first time in a Mediterranean coastal sequence.

2. GEOLOGICAL AND PHYSIOGRAPHICAL SETTING

The Balearic Islands constitute the emerged area of the so-called Balearic Promontory (Fig. 1), a mostly submarine relief stretching from La Nao Cape (East of Iberian Peninsula) to Menorca Island (NE extremity of the archipelago), (Ginés et al., 2012).

Formentera is the fourth island of the archipelago in surface area (82 km^2), and water depths between Formentera and Ibiza islands do not exceed 10 m, being this portion of sea occupied by several rocky islets, the biggest of which is *S'Espalmador*, separated from Formentera by waters shallower than 5m waters (Costa et al., 1985). Two former lagoons (*Estany des Peix* and *Estany Pudent*) have been preserved at the northern extremity of the island (Fig. 2), separated from the open sea by Upper Pleistocene sandy beach and dune barriers.

Most of the substratum of the island consists of Late Miocene carbonate rocks (Cabra et al., 2009), covered by Quaternary deposits, mainly of karstic (red decalcification clay) and aeolian (dune sand and aeolian silts) origin (Fig. 2).

The morphology of the island is featured by the occurrence of two large promontories, *La Mola* (197 m above sea level, asl) to the east, and *Barbaria* (108 m asl) to the west, the bulk of which are Messinian carbonates. A small 5 km long - 1.5 km wide NW-SE isthmus, less than 50 m in elevation connects both promontories (Fig. 2), being covered by Lower-Middle Pleistocene conglomerates and sandstones, rich in mollusc shell moulds, which represent marine terraces (perched 40-45 m asl) and cemented aeolian dunes (Cuerda, 1984). All these materials are mainly of calcareous nature, where an intense karstification has given place to a wide variety of cavities filled with reddish decalcified clays and aeolian silts (Cabra et al. 2009).

Two main fault systems, N20-40ºE and N120ºE are clearly visible in the island affecting the aforementioned Upper Neogene and Pleistocene deposits. Both systems display signals of Quaternary activity, however, is the N20-40º the one which holds a significant morphological expression, bounding the eastern and western promontories of the island (*La Mola* and *Barbaria*; Fig. 2). This fault system presents a dominant normal fault kinematics that gave place to a N-S graben-like trough where the NW-SE quaternary isthmus developed (Fig. 2). The recent activity of this fault system includes the deformation of the last interglacial to glacial sedimentary sequence of *Es Copinyar-Caló des Morts* (Goy et al., 2010). This sequence is in the south-western edge of *La Mola* at the hanging wall of *Es Ram* Fault (Fig. 1), outcropping along an outstanding sea-cliff topped by a littoral platform at +10-12 m asl. Several karstic gullies rooted in the dolomitized uppermost Miocene materials of *La Mola* constitute the main sedimentary source area of the studied sequence (Fig.2).

Nowadays Formentera presents a typical warm-temperate Mediterranean weather, with average annual temperatures of c. 18ºC, and maxima oscillating between 35-25ºC (day-night) in summer and 12-8ºC in winter. Rainfall is scarce and irregular, with mean annual values of c.350 mm, concentrated in winter, for which reason Formentera is considered the most arid island in the archipelago. On the other hand, the flat shape of the island favours an active wind dynamics with the most frequent winds blowing from E-NE and W-SW (Costa et al., 1985). Two maxima in this wind dynamics are reached in December-January, with prevailing northerly winds (NW: *mistral*, N: *tramuntana*, NE: *gregal*), and in April-May with easterly winds (*levante*). It must be noted that the location of the studied site with respect to *La Mola* massif is essential to understand the preserved pattern of paleowinds, as this promontory effectively shelters the site from winds blowing from the NE and partially from the SE. The astronomical tidal range in the Balearic Sea is about 15cm; annual sea surface temperature (SST) ranges between 18 and 19ºC, (Locarnini et al., 2013) and annual sea surface salinity (SSS) between 36 and 37 psu (Zweng et al., 2013).

The location of the Balearic Islands within the Western Mediterranean Circulation pattern (Fig. 1), in an intervening position between the cooler Catalonian-Provençal subbasin and the warmer Algerian one, is crucial for understanding the climatic and environmental characteristics of these islands, and hence its evolution since the Last Interglacial. In the Gulf of Lions, to the north, north-westerly winds induce the occurrence of cooler surface waters, while the Balearic Sea, protected by the Pyrenees, present warmer surface waters (Millot, 1999; Millot and Taupier-Letage, 2005). These contrasting sea surface temperatures define the so-called Northern Balearic Front, which shifts towards the south during colder seasons when the influence of northwesterly winds in the Gulf of Lions is higher, inducing warmer surface temperatures in the Balearic Islands. The southern sea of the islands is affected by the anticyclonic gyres of the Modified Atlantic Water (MAW; Millot, 1999) coming from the Alborán Sea.

3. METHODOLOGY

Standard field and sampling methodologies were employed to survey the best-exposed and most complete sections in Formentera Island. Conventional facies analysis was applied for the recognition and interpretation of sedimentary units and paleowind directions were measured and logged as paleoflow directions in all aeolian and marine units.

In the microtidal western Mediterranean domain, the plunge step marks the boundary between foreshore and shoreface (Bardají et al., 1990, Roep et al., 1998, Dabrio et al., 2011), so this sedimentary structure has been used to reconstruct ancient sea level positions. Measured elevations above present sea level are reported in this paper as, for instance, +1.5m asl.

3.1. Mapping

Geological and geomorphological mapping was obtained by means of air photographs scaled 1:30,000, with data represented on the 1: 25,000 map of the island (Fig. 2). Besides, a geo-referenced map was prepared superposing and integrating several thematic layers (contour lines, elevations and toponyms, all in vectorial format) upon the information of orthophotographs (air photographs) in raster format using GIS techniques (ArcGis v.10) applied to the Spatial Data infrastructure (IDEs) of the Regional Government of the Balearic Islands. Coordinate system and datum refer to GCS-WGS84, zone 31N.

3.2. Analysis of Sedimentary Units

The study of the sedimentary sequence (Fig. 3) included, besides a proper sedimentological analysis, petrography and palaeontology of the outcropping units. Standard petrographic analyses were carried out on thin sections from both the marine and the terrestrial units, under transmitted, polarized light after impregnation.

In the particular case of the marine deposits outcropping at the lowermost part of the sequence and some oolithic dunes from various outcrops of Ibiza and Formentera isalnds (Fig. 1), siliciclastic and bioclastic grains, as well as cementation and dissolution phases, were described. The aim of this analysis was to interpret these features within a sedimentological and morphological framework, and to compare them with other Upper Pleistocene deposits from the Iberian Peninsula (Zazo et al. 2003, Bardají et al., 2009).

Palaeontological analyses were focused on reviewing the existing data (Buzter and Cuerda, 1962; Cuerda, 1984; Gàsser and Ferrer, 1997; Gàsser, 1998, 2002), as well as collecting and classifying macrofauna from the marine deposits.

The study of the terrestrial units (Fig. 3) included mineralogical and geochemical characterization of deposits, magnetic susceptibility, analysis of soils and soil morphology, and phytolith content. Samples were collected along the uppermost 10 m of the section (Fig. 4), where sharp changes of sedimentary facies suggest an alternation between phases of aeolian activity with dune accumulation and soil development phases represented by sedimentary discontinuities.

3.2.1. Soil analyses

Description, sampling, and analyses of soils were carried out following the distinctive morphological, coloured and encrusted zones identified in the field survey. Colours are referred to Munsell Soil Colour Chart (1990). Standard soil sampling for textural, mineralogical and chemical analyses was carried out, as well as undisturbed samples for the micromorphological study of thin sections that were studied and described following the guidelines of Bullock et al. (1985).

The mineral phases of sediments and paleosols samples were determined by X-ray diffraction (XRD) at the Museo Nacional de Ciencias Naturales (MNCN, Madrid). Powder XRD patterns were obtained using pressed powder mounts employing a Philips semi-automatic PW 1710 diffractor producing monochromatized CuK α radiation. In addition, the <63 µm fraction of paleosols samples was routinely analysed in oriented aggregates in order to discriminate the main clay mineral species.

Geochemical analyses were carried out at the General Service of Applied Chemical Analysis (*Servicio General de Análisis Químico Aplicado*), University of Salamanca. Major and trace elements in total sediment samples were identified with an ICP- OES, after a microwave-assisted digestion with HNO_3 and HF [Gill (ed.), 1997; Lewis and McConchie, 1994; Murray et al. 2000].

3.2.2. Magnetic susceptibility

Dry samples were collected for analysis of magnetic susceptibility. Samples were disaggregated, packed firstly in plastic film and then into pre-weighed plastic cups and sealed with plastic caps. Low- and high-frequency (0.47 and 4.7 kHz) magnetic susceptibility were measured with a Bartington MS2 susceptibility meter single-sample sensor. All measurements were recalculated in relation to the weight of the sample to obtain a set of parameters and quotients: *Magnetic susceptibility* (χ), corresponding to the low frequency ($_{LF}$) magnetic susceptibility; χ_{HF} (high frequency magnetic susceptibility), χ_{FD} and $\chi_{FD\%}$ (frequency dependent magnetic susceptibility expressed as the difference between χ_{HF} and χ_{LF} as a mass-specific value and a percentage of χ_{LF}: $100(\chi_{LF}-\chi_{HF}/\chi_{LF})$.

3.2.3. Phytolith extraction and analyses

Phytolith assemblages related to present vegetation cover and soils were surveyed in order to compare with samples of various Pleistocene deposits.

Phytolith extraction from botanical samples followed the dry ashing methodology outlined by Albert and Weiner (2001) and summarized by Parr et al. (2001). A total of 18 plant species were sampled, representative of the vegetation associations in the study area: *Pinus halepensis* Mill, *Pinus pinea* L., *Juniperus phoeniceae* L., *Juniperus oxycedrus* L., *Pistacia lentiscus* L., *Cistus albidus* L., *Rosmarinus officinalis* L., *Chrithnum maritinum* L., *Olea* sp., *Coridothymus capitals* L., *Tamarix* sp., *Ammophila arenaria* L., *Cistus clusii*, *Ononis natrix* L., *Juncus* sp., *Atriplex rosea* L., *Salicornia* sp, *Suaeda fructicosa*. Stems, leaves, inflorescences and seeds were processed separately. Soil samples directly related to each association were also collected, processed and analysed. The percentage of each morphotype per species was calculated and types were described according to the descriptors of the International Code for Phytolith Nomenclature 1·0 (Madella et al., 2005).

Phytoliths were extracted from dry sediments (34 samples) of the sedimentary sequence, following the protocol summarized and adapted from Madella et al. (1998), and without fractionating due to the general characteristics of the sampled sediments (silt and fine sands). This procedure allows a recovery from the bulk sediment of a higher number of individuals without losing during the process the morphotypes with a size below 20 µm (which comprehends most of the phytolith sizes recovered). A weighted part of the final AIF (Acid Insoluble Fraction) sediment was then placed in slides (76x26 mm) and mounted with Canada balsam. A Leica DM 2500P, with a digital camera Leica DFC 420C, was used for the phytoliths counting and other biominerals study.

3.3. Chronology

The geochronological framework was established by integrating the luminescence dating (both Optically Stimulated Luminescence, OSL, and Thermoluminescence, TL), with the faunal assemblage found in the associated bioclastic marine deposits and oolitic facies, which are chronostratigraphic indicators of the Late Pleistocene (MIS5e) in the south-eastern coast of the Iberia Peninsula (Zazo et al. 2003, Bardají et al., 2009).

Samples collected for OSL dating of the oolitic facies from South Ibiza and Formentera (Fig.1) did not provide suitable results due to lack of OSL signal.

Ten samples were collected for OSL in Es Copinyar cliff section (Figs. 3, 4) in 2004 (FM04-3 y FM04-4) and 2009 (FM09-28, FM-09-15, FM09-16, FM09-13, FM09-11, FM09-09, FM09-10), and analysed following standard protocols in the Laboratoire des Sciences du Climat et de l'Environment (LSCE/IPSL, UMR CEA-CNRS-UVSQ at Gif sur Yvette, France), and Universidad Autónoma de Madrid (UAM, Spain) respectively. These laboratories calculated the dose accumulated by quartz grains using single aliquot regenerative-dose (SAR) and accumulated (additive) dose rate protocols respectively. Additionally, three new samples were collected for TL at the same section (FM12-01, FM12-02, FM12-03; Figs. 3, 4) and analysed in the Quaternary TL Surveys (UK). TL dating procedure involves evaluation of the *paleodose* and dose-rate assessments of the samples. Sediment samples were collected at 10 cm above and below each TL sample, and the gamma dose-rate assessment was based on data from all three samples. The cosmic radiation dose-rate was estimated from the burial depth of the TL sample. The dose-rates have been corrected to allow for the estimated past moisture levels in the sediments, and the error limits include uncertainties in these estimates. The TL ages presented include corrections for the decay of the TL signal, and they refer to the most recent exposure to daylight of the fine-grained fraction of the sediment. The error limits of TL dates include random and systematic uncertainties in laboratory measurements and environmental factors and refer to a 68% confidence level. Within the measurement error limits, the TL dates are consistent with the assigned stratigraphic position of samples and sediments.

4. RESULTS

4.1 Sedimentary record of Es Copinyar– Caló des Morts section

The cliff between Es Copinyar and Caló des Morts (Fig. 3) displays the most complete and continuous sequence of marine and terrestrial units in the island, representing the last interglacial-glacial cycle.

4.1.1. Marine Units

Three marine units (MU), separated by erosional surfaces, outcrop at the base of the Es Copinyar – Caló des Morts sequence (Figs. 3, 4): MU-1a) Tectonically deformed microconglomeratic unit, with some oolites and warm Senegalese fauna; MU-1b) Conglomeratic unit, with some oolites and bearing warm Senegalese fauna; MU-2) Bioclastic sands with reddish matrix, rich in *Glycymerys* shells.

Pleistocene activity of Es Ram fault zone (Fig.2) triggered an apparent large scale decametric folding and eastward tilting (10-15º SE) of the complete marine sequence (MU-1 and MU-2; Fig. 3). A clear and repetitive upward folding is observed in the basal marine unit MU-1 (a, b), roughly parallel to the present shoreline trend (NW-SE), with fold axes nearly parallel to the fault system (N20ºE). This deformation pattern seems to be generated by repeated synsedimentary normal faulting and back-tilting of the Miocene substratum between Es Copinyar (West) and Punta de sa Fragata (East) and the subsequent adaptation of the softer sedimentary cover by folding and tilting (Es Ram site; Fig. 2). This deformation style (antiforms or synforms) causes the sedimentary sequence to occur successively above or below the present sea level all along the studied zone.

Marine Unit 1a (MU-1a)

The oldest Pleistocene deposits (MU-1a; +1-1.5m amsl) lay unconformably over the Late Miocene basement. This unit consists of a highly cemented marine bioclastic limestone with grain sizes ranging from coarse sand to microconglomerate (grainstone to rudstone) that preserve a seaward-inclined parallel lamination corresponding to the upper shoreface - foreshore (Fig. 5A). The uppermost part of this unit is affected by polygonal sandcracks (Fig. 5B).

Thin section analyses (Fig. 6 A, B and C) show that this unit is mainly constituted by rounded skeletal remains of molluscs, echinoids, calcareous algae and crustacean microcoprolits (*Palaxius?),* and coarse-grained carbonate rock fragments. These rock fragments correspond to reworked oolitic calcarenites (c. 12%) the source of which must be discussed, and underlying Tortonian carbonates. Some particular features are the presence of thin tangential aragonite coatings, resembling coarse oolitic grains, in rock fragments and bioclasts (~15%), as well as oolitic aggregates. Two phases of submarine cementation: a first micritic one and a later prismatic sparite have been also identified (Fig. 6B).

Besides the deformation caused by the N20ºE fault system above mentioned, this unit is also affected by two systems of joints, oriented N60ºE and N140ºE.

Marine Unit 1b (MU-1b)

A second marine unit (MU-1b) develops at the foot of a low cliff (0.5-1m high amsl) carved into the previous marine unit MU-1a (Fig. 5A). This younger unit consists of a highly cemented conglomerate with reworked boulders of MU-1a (Fig. 5B), which also appears filling erosive potholes carved on MU-1a. The faunal content and the matrix of this boulder bearing deposit are similar to the first marine unit (MU-1a). Petrographic analysis shows also a high skeletal content but almost no aragonite coatings or ooliths. Cementation features have been identified (Fig. 6D), with prevailing blocky over prismatic cements.

The faunal content of Marine Units MU-1a and MU-1b includes the termophilic species (Senegalese fauna) *Strombus bubonius* (Fig. 5C) and *Conus testudinarius*, suggesting a Late Pleistocene age (Gàsser and Ferrer, 1997; Gàsser, 1998), as well as more common species in the Mediterranean such as *Stramonita haemastoma, Acanthocardia tuberculata, Arca noae, Cerithium vulgatum* and *Glycymeris violascescens,* among others. A total of 23 mollusc (9 bivalves, 14 gastropods) species have been described for this deposit related to coarse sand and rocky shores environments (Cuerda, 1984; Gàsser and Ferrer, 1997; Gàsser, 1998). The petrographic analysis of thin sections (Fig. 6) reveals the occurrence of other marine species from coastal and shallow shelf environments such as echinoderms (*Paracentrotus lividus*), crustacean decapod species, and coralline algae (*Amphiroa sp.* and unidentified fragments).

Marine Unit 2 (MU-2)

A third, younger, marine unit (about 1.8m amsl; MU-2) constituted by a poorly cemented layer of reddish *Glycymeris*-rich sandstone, develops above an erosional surface onlapping previous units. On the western part of the section, the upper surface of this layer is crisscrossed by polygonal cracks, very much resembling retraction cracks, which are partly filled by reddened material from the overlying deposits (Fig. 5D).

The faunal content is characterized by abundant *Glycymeris violascescens* and few other species (*Acanthocardia tuberculata, Stramonita haemastoma,* among others; Gàsser, 1998). The mollusc species preserved on this unit (5 bivalves, 6 gastropods) are also related to coarse sandy and rocky shores environments and suggest a Late Pleistocene age (Gàsser, 1998). The petrographic analysis and samples also reveal the presence of other marine species, common in the coastal and shallow shelf environments such as echinoderms (*Paracentrotus lividus*), crustacean decapoda species, and coralline algae (*Amphiroa sp.* and unidentified fragments).

The internal organization and faunal content, closely resembles the present-day storm deposits and *Glycymeris*–rich beach found nowadays at the upper foreshore and storm berm in the backshore in this same area (Fig.7).

4.1.2. Terrestrial Units

On top of above-described marine units, up to six terrestrial units have been identified constituted by different generations of aeolian dune systems and scattered scree deposits. Soils developed among aeolian phases have been also described and analysed.

Terrestrial Unit 1 (TU-1)

This lowermost terrestrial unit consists of a sandy-silty layer, c. 90 cm in thickness, which fills the retraction cracks at the top of the underlying *Glycymeris*-rich MU-2 (Fig. 3, 4).

It is organized in three layers with somewhat diffuse limits (Fig. 8). The lower one is a weakly cemented brownish sand bed with scattered *Glycymeris* and other mollusc shells, as well as some angular carbonate fragments. A yellowish red middle layer is poorly visible because bioturbation; it locally contains scarce, scattered mollusc shells in the lower 10 cm. The upper layer is a reddish clayey unit, with accumulations of angular pebbles of Miocene carbonates and cemented Pleistocene aeolianites. They occur as laterally discontinuous beds with erosional bases and irregular tops. The lateral extent rarely exceeds a few meters, and thickness is generally lower than 15 cm, although some coarser clasts are often larger than the average thickness of a given individual layer. Other layers are simply lines of pebbles.

Soil morphology shows a Ck-2Bw-2BC-3C horizon sequence (Fig, 8; Table I), with colour gradually changing from reddish brown (2Bw-2BC; 5YR 5/4 - 2,5 YR 4/4 m) to yellowish red (C; 5YR 4/6 m) from top to bottom. Field description shows that these horizons are slightly plastic and adherent, structureless and with traces of some fine and very fine roots, sometimes calcified.

Organic matter never exceeds 1%, but as occur with clay content, it also increases with depth, reaching a maximum at 30cm, what suggests a somehow long stabilization period that favoured pedogenesis. The increase in clay content cannot be interpreted as a result of illuviation due to the high $CaCO_3$ content (Table I) that prevents dispersion of clay particles previous to their translocation, and by the lack of micromorphological evidence of illuviation; however, it cannot be absolutely ruled out at least during the early stages after deposition. Decalcification of parent material, such as the *terra rossa* from karstified Miocene materials, could favour an early moderate clay migration later masked by carbonate leaching from the overlying dune deposits. Crystallithic b-fabric in the reddish groundmass suggests recalcification linked to carbonate leaching from overlying calcareous dunes.

Other inherited properties from source area are rubefaction and illite (micas) content, although rubefaction could also have increased later during younger stages of hydric stress (water deficit). Finally, shells and calcite grains constitute the coarse fraction.

The whole unit is interpreted as an alluvial deposit fed by sandy-silty material eroded from the karstified La Mola relief and moved down slope as sand-rich mudflows and debris flows responsible of the chaotic arrangement of clasts, and the relatively narrow tongues; flash floods moved coarse grain-sizes forming thin layers of pebbles that occur as clast lines in cross section. The presence of scattered *Glycymeris* and other mollusks shells in the lower weakly cemented brownish sand bed may point to a close but receding sea level.

Terrestrial Unit 2 (TU-2)

Terrestrial Unit 2 (TU-2) consists of a white, partly cemented and well-sorted medium to coarse sandstone, made up of skeletal fragments (bioclasts) of molluscs, echinoids and calcareous algae, pellets and reworked oolites (less than 10-15%). The internal structure is a large-scale high to moderate angle tabular cross bedding (visible thickness, at least 7 m), which is exposed c. 200 m in downwind direction (Fig. 5D). It is interpreted as a transverse aeolian dune that migrated towards the south under prevailing northerly winds. The orientation of the outcrop barred further observations concerning the type of dune.

OSL ages (FM04-3; 72±7 ka BP) indicate that the dune accumulated during MIS 4, in areas not far from the shore, given the abundant bioclasts which are clearly derived from coastal settings. The absence of bioturbation by plant roots suggests that the large dune migrated freely, and climate was not favourable for plant colonization. The low topography of the area allowed sediments originally deposited on the northern coasts of the island (reworked oolites) to be mobilized across the low-lying strip of land to be finally accumulated in aeolian sand dunes at the southern toe of La Mola promontory, which shelters this site from north-easterly and easterly winds.

Terrestrial Unit 3 (TU-3)

After deposition of TU-2, an erosional phase promoted the excavation of a deep incision surface down to the cemented MIS 5e (MU-1) marine deposits (Fig. 3; Fig. 9). The surface dips towards the S/SE, partly out of the cliff wall, so the dip observed along the cross section is only apparent. Angular carbonate pebbles and boulders found near the incised surface witness that erosion affected the older lithified dune deposits cropping out at higher topographic elevations. Locally, towards the deeper part of the incision surface, the accumulation reaches up to 20-30 cm in thickness and can occur as matrix-supported conglomerate with reddish sandy-silty matrix, interpreted as scree deposits.

The bulk of TU-3 is white medium to coarse bioclastic sand with variable cementation. Mineralogy is calcite (40-60%) and aragonite (35-37%), with minor contribution of quartz (3%). The internal structure is large-scale cross bedding, with at least two large sets exposed in the outcrop (Fig. 10A) migrating in opposite directions. The older one is tabular with rectilinear to gently sinuous crest, which migrated to the S/SSW under prevailing northerly winds, partly fossilizing the afore mentioned erosion surface (Fig. 9; Fig. 10A). No bioturbation has been observed and it is cemented. The upper set is trough cross-bedded, less cemented and intensely bioturbated by plant roots (Fig. 9A; Fig. 10B), some of which relatively large sized. The preserved thickness is c. 2 m, being laterally continuous for more than 300 m in down-current direction (NE; Fig. 10A). OSL ages (FM04-4, FM09-28; 54±5 ka BP, 51±4 ka BP) indicate accumulation during OIS 3.

The erosional surface on which TU-3 accommodates is interpreted as the consequence of a major drop of base level, during a lowstand of sea level, which was later fossilized by aeolian dunes, with variable sources of sediment supply. Initially, large dunes migrated from the north crossing the narrow island, high sand supply and relatively constant northerly winds account for the straight crested morphology of the dune. Later, prevailing winds rotated to the southwest and supplied less amounts of sediments, which accumulated in barchanoid dunes. The increased abundance of plant roots suggests a moister climate that presumably accounts for the diminished sand supply.

Terrestrial Unit 4 (TU-4)

Terrestrial Unit 4 develops on top of a gently irregular erosion surface carved onto TU-3 (Figs. 3 and 4), which is overlain by a thin accumulation of irregular, angular lithified clasts of older aeolian dunes, more abundant in the topographically lower parts of the surface (Fig. 10B) interpreted as scree deposits. Increased cementation of the surface produces a morphological platform noticeable along the sea cliff (Fig. 3).

The mineralogical composition of TU-4 shows a clear predominance of aragonite and magnesian calcite (Table II). The internal structure is largely obliterated by the intense root bioturbation present in the uppermost part of the outcrop (Fig. 10C). Looking in detail, remains of a low angle cross-stratified unit, with thick foreset laminae gently dipping to the east, are preserved in the south-eastern part of the outcrop, being overlaid by a coarser clastic cross bedded unit (Fig. 10B). Sets of parallel laminations predominate in the central portion. Cross bedding pointing to the N-NE and E, and parallel lamination, both crossed by large plant roots which are better preserved at the north-western end of the cliff. Relict locust egg pods are frequent in the southern part of the outcrop. A very weak cementation makes this unit to be easily removable by weathering. Terrestrial gastropods (*Helix sp*) have been collected in the upper part.

TL ages (FM12-03; 86+25/-16 ka BP) gave unsustainable error ranges, but according to OSL ages (FM09-15; c. 53±5 ka BP) this unit should have accumulated during MIS 3.

The observed arrangement of sedimentary facies (Fig. 3) is interpreted as the accumulation of low climbing dunes (SSE) attached to the lower slopes of La Mola. These changed laterally to interdune deposits dominated by deflation (centre of the section), and, towards the NW, to small dunes that covered topographically more-elevated areas, at the top of the cemented, exhumed remains of TU-2. We assume that the local water table played a major role allowing more vegetation and invertebrate life in the topographically lower parts of the outcrop, where reddening is also more prominent.

Terrestrial Unit 5 (TU-5)

Although its lower boundary is irregular and somewhat diffuse, TU-5 stands out of the cliff because of the presence of more resistant calcareous levels and colourful layering (Fig. 3). This unit shows two clearly distinguishable parts (Figs. 10B, 11). The lower part (TU-5a in Fig.11) consisting of yellow to reddish silty sands, with irregularly scattered angular pebbles of older cemented aeolian dunes, some of which may reach more than 10 cm in length (major axis). The internal sedimentary structure of the upper redder interval is obscure, masked by intense bioturbation by plant roots and locust egg pods, whereas carbonate clasts and removed egg pods tend to occur as irregular layers mostly in the lower yellowish interval where they can be traced laterally several tens of centimetres to a few meters.

An irregular erosion surface separates this lower part from the upper one (TU-5b in Fig. 11), easily traced along the entire outcrop, and marked by a few centimetres thick calcareous crust and plant roots concretions that make the boundary to protrude out of the cliff wall. The organization of this upper part is more complex as compared with the lower one, being intensely bioturbated by locust egg pods and plant roots, most of which are more cemented than and clearly discernible from the hosting sediment. There are also irregular layers of pebbly sandstone/mudstone with lithoclasts derived from eroded aeolianites and Miocene carbonates. Besides, there are frequent irregular erosion surfaces, hardened by cementation, and many of them covered with irregular lithoclasts with little finer matrix, and remobilized locust egg pods. Imbrication of such surfaces towards the top contributes to form a hard horizon, very conspicuous in the cliff. Terrestrial gastropods (*Helix sp*) and locust egg pods similar to those described in Canary Islands by Alonso-Zarza and Silva (2002) are abundant.

Three pedo-sedimentary cycles have been described in this unit (I, II, III in Fig. 11; Table I), separated by few centimetre-thick undulated and irregular calcareous crusts. Upper sandy deposits (Cycle I) change gradually from brown (7,5YR 6/4d) to light yellowish brown (10YR 6/4d) colours, overlapping a pale brown (10YR 6/3 d) few centimetre-thick irregular level (Cycle II) limited by indurated crust, below which a reddish yellow (7,5YR 6/6d) to pink (7,5YR 7/4 d) deposit (Cycle III) appears.

All three cycles show a weak pedological development, with little evidences of soil forming processes (Table I), and only the intermediate cycle (II) standing out by its darkening linked to the organic matter content and lower values in calcium carbonate (Table I). The high calcium carbonate content in some horizons, near 80%, coinciding with high sand proportion (Table III), likely indicate a detrital source instead of pedogenic origin to these limy accumulations, because calcium carbonate precipitation usually tends to concentrate in silt fraction.

Calcite prevalence (80%) together with aragonite features mineralogy in all cases (Table II).

Variable amounts of quartz and micas (Table II) present in the upper parts of each cycle are interpreted as due to fluvial input inherited from source area (supported by higher Mg/Al ratio, suggesting higher humidity (moisture). Regarding the geochemical results (Table III), the higher Al_2O_3 and K_2O content in the upper horizon (samples j, k, l in Table III) confirms the clay minerals presence (mainly illite), as well as Fe_2O_3, related to a high magnetic susceptibility, is associated to the presence of ferromagnetic minerals.

According to OSL ages (FM09-16, FM09-14; c.48±3, c.40±2 ka BP), accumulation of TU-5 took place during MIS 3. TL ages are consistent with these results (FM12-01; 48,2 +8.1/-6.6 ka BP)

TU-5 is interpreted as an intensely bioturbated, mass-flow dominated colluvium deposited at the base of La Mola, which underwent successive phases of plant colonization and pedogenesis, with associated development of carbonate crusts towards the upper part. The occurrence of imbricate, shallow troughs towards the top, suggests an episode of more humid conditions with a significant vegetal cover, a network of divagating shallow channels that drained La Mola, and occasional mass flows.

Terrestrial Unit 6 (TU-6)

TU-5 is crowned by a centimetre scale calcareous crust, which is eventually broken into heterometric angular flat pebbles. A new mass flow dominated colluvial unit (TU-6, Figs. 3, 4, 10) develops over this hardened surface incorporating fragments of the calcareous crust in its lower part, as well as egg pods and terrestrial snails (Fig. 12). The sedimentary characteristics (poorly organized heterometric, matrix-supported breccia, poorly organized) indicate that accumulation of TU-6 must have taken place during a relatively humid period, after the aridity marked by the lower calcareous crust.

The soil developed on these materials displays the following horizon sequence C-2Ck1-3Ck2 overlying the lower calcareous crust (3Ckm3) (Table I; Fig. 12). There are slight differences in colour between the brown upper horizons (brown (7,5YR 5/4 w) and lower light brown horizon (7,5YR 6/4w), the most outstanding feature of which is a higher content of coarse fragments content increasing laterally from 10% to 30%, without marked differences in other textural fractions (Fig. 12; Table I).

Leaching and translocation of calcium carbonate are the main pedogenic processes, with calcium carbonate content increasing with depth and reaching values of up to 86%. These carbonate accumulations form a few centimetres thick crust at the base of the profile (3Ckm3; Fig. 12).

Mineralogy (Table II) is characterized by calcite prevalence together with aragonite and slight variations in quartz content. Illite (micas) is likely inherited from parent material as happened with soil developed in TU-1, whose source area is mainly the *terra rossa* resulting from karstification of Miocene materials of La Mola.

An erosional flat surface carved on this unit constitutes the top of the present cliff (Fig. 10E). This surface is sporadically affected by polygonal retraction cracks (Fig. 10F) and implies a very important gap in sedimentation, suggesting a long-lasting exposition to extreme arid conditions which could have favoured wind deflation, desiccation and cracking.

According to OSL/TL ages, the age of this unit is bracketed between 20±2 ka BP (FM09-13) and 17+2.4/-2.2 (FM12-02).

Terrestrial Unit 7 (TU-7)

This upper unit consists of large scale, cross-bedded, well-sorted medium to coarse sand and sandstones. The lower part is cemented with variable bioturbation by plant roots (Fig. 10 B, D, E and F). The unit is interpreted as aeolian dunes that migrated under the influence of persisting northerly winds crossing the narrow land strip that connected La Mola with the rest of the island. OSL age (FM09-11; 19±1 ka BP) indicate accumulation during the end of LGM, when rising sea level and deteriorating climate increased the sand supply in the northern side of the island and vegetation colonized the dunes in the more distal (southern) parts.

A younger system of uncemented aeolian dunes covers the former deposits (Fig. 10F). Layers of bioturbated grey sand, a few centimetres thick, separate individual dunes, which are partly fixed by vegetation. OSL ages (FM09-09, FM09-10; 16±1, 14±1 ka BP) indicate that this is a relatively old system that also migrated from the northern part of the island.

There are still more recent dune systems, not included in this work, which are not cemented and partly fixed by vegetation.

4.2. Magnetic susceptibility

Magnetic susceptibility values along the sequence (Fig. 13) show that higher peaks occur within the reddish terrestrial non-aeolian units (TU-1, upper TU-5 and TU-6). These magnetic susceptibility peaks are related to higher contents in Al, Fe, Mg, K and Ti (Table III).

The highest peak occurs at 1.5-2 m, within the TU-1 (samples γ3, γ4 in Fig. Fig. 13), which can be associated to *in situ* pedogenic processes as well as inherited from “terra rossa” from karstified Miocene materials. Peaks in TU-5 seem to be associated to incipient pedogenic processes (+8.1m; sample j in Fig. 13) or to colluvial origin (+7.25m; sample e in Fig. 13) when sedimentological characteristics (presence of small channels, pebbles and coarse sands) so point it. The upper peak (unit TU-6; +9.5m; samples q in Fig. 13) is clearly related to the abundance of ferri- and ferromagnetic materials. Most of the upper aeolian unit (TU-7) shows very low magnetic susceptibility (as correspond to diamagnetic minerals, such as quartz and calcite), except for a slight peak (+15.4m; sample w) that can be related with a sedimentation stop and incipient pedogenic processes in the aeolian sediments.

The higher concentration of magnetic materials in paleosols is related to its finer grain size while this concentration is much lower in coarser aeolian deposits (Kukla et al., 1990; Heller et al., 1991). Magnetic susceptibility values obtained in coeval deposits form Mallorca (Nielsen et al., 2004) are higher in colluvial sediments than in aeolian ones, with marked peaks being related to humid periods whereas low susceptibility values corresponding to arid conditions. Although the causes of magnetic susceptibility variations are still a matter of debate, some authors (Zheng et al., 1990, Maher, 1998) suggest that magnetic materials may form during soil development in warm and humid periods while low susceptibility values found in aeolian deposits are related to arid periods.

4.3. Phytoliths analyses

The analysis of plants and soil samples allowed the identification of four distinctive assemblages (with diagnostic phytoliths) corresponding to four vegetation type sites: a) wooded dunes, b) dune shrubland, c) dune/intradune vegetation, and d) halophytic meadows (Fig. 14). From the 18 plant species identified, 10 were found to produce uniquely shaped phytoliths (*Pinus halepensis* Mill, *Pinus pinea* L., *Juniperus phoeniceae* L., *Juniperus oxycedrus* L., *Pistacia lentiscus* L., *Rosmarinus officinalis* L., *Olea* sp., *Tamarix* sp, *Ononis natrix* L., *Juncus* sp.*).* In the case of the grass vegetation (halophytic meadows, and dune/intradune colonization sites), although the plants analysed share multiple common phytolith type morphologies, the halophytic species, namely the *Juncus sp., Salicornia sp. and Suaeda fructicosa,* produced a high number of calcium oxalate biominerals of the raphide and, most commonly, druse types (*Juncus sp*.). The druse types phytoliths are related with plant growing under conditions of water stress.

Although all soil samples from the four vegetation type sites present a large number of non-diagnostic phytolith morphologies and types, diagnostic phytolith groupings were identified, including: a) smooth polyhedral, tracheary forms and cylindroid types, in the wooded dunes sites, b) cuneiform, acicular, tabular scrobiculated, trapeziform sinuate, and trapeziform short cell types in the dune shrubland, c) trapeziform polylobate, cuneiform short cell, bilobate asymmetric, long saddle and parallepipedal short cells in the Dune/intradune vegetation sites and d) elongate sinuate, tabular scrobiculated, saddles and druses and raphides of calcium oxalte in thehalophytic meadows.

On the whole, the content of fossil phytoliths was poor, with 19 out of the 34 samples found to be sterile (Fig. 14). The overall counting is low and its presence in the sediments is associated with evidence of bioturbation related to vegetation cover. Preservation along the stratigraphic sequence is clearly uneven. Although no studies have been made till date regarding phytoliths preservation in these environments, the non-existence of phytoliths and other plant biominerals in sediments with signs of bioturbation could be linked to pH and time. Lasaga (1984) indicates a preservation age (at a pH~4) of phytoliths in non-cohesive sediments and soils between 25.000 and 250.000 years. The strong surface dissolution observed in the few phytoliths recovered within the lower sedimentary units (TU-1 to TU-5) would corroborate this hypothesis.

Phytolith morphotypes associated with grass plant families are largely the most common types of morphotypes (Fig. 14), whereas shrubs and trees phytolith counting account for 13% of all the diagnose-morphotypes identified.

The sample collected at the top of the TU-5 yielded a significant lower number of phytoliths than the two samples from TU-6, also with signs of bioturbation. The morphotypes correspond mostly to halophytic vegetation. In the samples collected for mineralogical study, calcium oxalate biominerals were also found, mainly druses, which indicate a marked xerophytic character of the vegetation at the end of this stage, and prior to the establishment of relatively wetter conditions recorded at unit TU-6.

Samples collected at unit TU-6 presented the highest number and diversity of morphotype phytolith. A higher percentage of *Poaceae*, *Fabaceae* and *Lamiaceae* associated morphotypes, as well as the presence of polyhedral scrobiculate and cuneiform forms, and the presence of the only globulate echinate morphotypes (*Palmae sp.*) suggest the colonization with predominantly non-halophytic grasses, and the presence of fresh water (*Palmae sp.*) during the deposition of this unit.

The phytolith analyses of the samples collected along the upper unit (TU-7) suggest a progressive aridity with an increase of the salt-tolerant grass species with the maximum halophytic grass colonization registered towards the top of the sequence. Phytolith analyses of the two upper samples indicate a decrease in salt tolerant grasses, which could indicate less arid conditions.

5. DISCUSSION

The coastal sedimentary sequence studied in this work covers the time span between ca. 130 ka BP and ca. 14 ka BP (MIS 5 to MIS 2). The sequence records on the one hand the sea-level changes occurred through MIS5, and on the other hand, a complex paleoenvironmental history that can be related to oceanographic and atmospheric changes in the North Atlantic region along the last 80ka.

Paleoclimatic reconstructions in Mallorca Island over the last 140 ka (Rose et al., 1999) show major changes in mean annual temperature and wind regimen, with the most important rates of geomorphologic change occurring during periods of climatic deterioration with reduced vegetation cover. Evidence of changes in effective precipitation has been deduced from the growth history and δ^{13} C in a littoral karstic speleothem in Mallorca (Hodge et al., 2008), where sub-millennial climate shifts occur between c.112 and c.48 ka, i.e. from the final part of MIS 5e to MIS 3.

Late Pleistocene carbonate aeolianites have been usually related to glacial or stadial arid periods with low sea level (Rose et al., 1999; Clemmensen et al., 2001; González-Hernández et al., 2001, Fornós et al., 2008), occurring in alternation with colluvial deposits and paleosols developed during relatively humid climate intervals. A millennial scale interestadial/stadial climate alternation has been recognized from the dynamics of cliff-front aeolian and colluvial systems (Clemmensen et al., 2001). Fiol et al. (2005) proved that dust rains and dust deposition play a significant role in Balearic Islands. The role of African dust in the formation of Quaternary red soils and paleosols in Mallorca has been more recently analysed by Muhs et al. (2010). The study of fluvial sequences in the Mediterranean basin (Macklin et al., 2002) over the last 200 ka, show that rapid and high- frequency climate changes in the North Atlantic during the last glacial period had a profound climate effect not only on the vegetation of the Mediterranean real but also on catchment erosion and river alluviation. Late Pleistocene alluviation occurred during cool and dry stadials when steppe vegetation replaced forest or wooded steppe biomass. This work is thus a contribution to the understanding of how climate has evolved in this sensitive area of Western Mediterranean along this time period.

5.1. Sea level highstands during MIS5

The first stratigraphic studies of Quaternary deposits in Mallorca and detailed paleontological investigation (Butzer and Cuerda, 1962; Cuerda, 1989, and references therein) turned Mallorca in a key site for the study of the Last Interglacial (“Tyrrhenian”) in the Mediterranean. Research in Mallorca has incorporated diverse dating methods: U-Th and AAR (Hearty, 1987), U-Th (Hillaire- Marcel et al., 1966; Goy et al., 1997; Zazo et al., 2003; Muhs et al., 2015) in marine terraces, and U-series measurements in phreatic speleothems of littoral caves (Ginés et al., 2005, Tuccimei et al., 2006, Dorale et al., 2010; Ginés et al., 2012). These results allowed a more precise chronology of sea level changes during MIS5, with sharp, millennial-scale fluctuations of almost 20m (including highstand, intervening lowstand, and succeeding highstand) within the peak of the Last Interglacial *s.s.* or MIS 5e (Tuccimei et al., 2006).

However, Last Interglacial marine deposits are not so well known in other Balearic Islands. In Ibiza Island, the record of MIS5e is scarce and consist mainly on erosive morphologies such us platforms and notches (Punta des Farelló), or remains of beach deposits with banal marine fauna (Cala Gració, Cala Xarraca; Cuerda, 1984), with maximum elevations reported at +2-2.5 m. Detailed paleontological studies, and first *in situ* descriptions of the termophilic species *Strombus bubonius* and *Conus testudinarius* (Senegalese fauna) were described by Gàsser and Ferrer (1997) and Gàsser (1998). In Formentera, the record is even more scarce, with only small patches of MIS5 sandy beaches having been described around the island (Vicens et al., 1992; del Valle et al., 2020; 2021).

In the Mediterranean peninsular coast of Spain, MIS 5e is characterized by oolitic beaches and dunes witnessing suitable environmental and climatic conditions for the development of oolitic shoals (Zazo et al., 2003; Goy et al., 2006; Bardají et al., 2009). Oolites from the Last Interglacial in SE Spain are generally spherical or ovoidal, fine medium grained (100-400 μm), with thin laminated tangential aragonitic cortex. These types of oolites are usually formed in shallow-marine carbonate saturated shallow waters, with a constant agitation under the influence of tidal currents or wave action (Wanless and Tudesco, 1993; Flügel, 2010). According to Bardají et al. (2009), prevailing SE winds favoured the accumulation of these oolitic beach-dune systems in SE Iberian Peninsula during OIS 5e.

In Balearic Islands, the scenery is quite different with oolitic units only observed in Formentera and in the south of Ibiza. The highest oolitic content is observed in the northern Formentera dune-systems, at Ses Illetes and in a much lesser extent in the south of Ibiza. Two episodes of oolitic dune accumulation, separated by a sharp deflation surface, have been described on the central part of Formentera and in the south of Ibiza (Goy et al. 2007). The oolitic dune systems in Ibiza and Formentera Islands accumulated under prevailing W-NW winds, but the associated oolitic beaches do not crop out above present sea level. Location of these dunes and oolite features point to the presence of an extended platform connecting Formentera and Ibiza, where warm and carbonate saturated shallow waters, constant winds and water agitation, low clastic sediment supply to the coast and few or none coral-reefs and/or algae colonization of the platform, provided the ideal environmental conditions for oolite development probably at the beginning of the first highstand of MIS 5e. Besides that, the high content on crustacean decapods coprolites found in these dunes suggests that these environmental conditions were suitable for the activity of the crustacean, and for the preservation of these particles.

Two marine units, showing at least three sea level hisghtands, constitute the base of the studied sequence (Figs. 3, 4 and 5). Their attribution to MIS5 is based on petrographic characteristics, faunal content and stratigraphic relationships with the rest of the sequence. The oldest unit (MU-1a) lays unconformable over the Late Miocene basement. It is a highly cemented marine bioclastic calcarenite with grain sizes ranging from coarse sand to microconglomerate (grainstone to rudstone) that preserves the seaward dipping lamination corresponding to the uppermost foreshore. Rounded skeletal remains (bioclasts) of molluscs, echinoid and calcareous algae, fecal-pellets and coarse-grained carbonate grains (rock fragments) are observed in thin section. Carbonate rock fragments derive mainly from reworked oolitic calcarenites (c. 12%) and underlying Miocene carbonates. Some rock fragments and bioclasts incorporate tangential aragonite coatings (~15%), resembling coarse oolitic grains. The presence of reworked fragments of oolitic calcarenites and their petrographic characteristics points to the existence of an oolitic beach nearby, possibly located below present sea level, since cementation degree, composition and grain size are not compatible with the emerged oolitic dunes. A second, younger, marine unit (MU-1b) accumulated against a degraded small cliff (0.5-1m high) carved into MU-1a (Fig. 5). It consists of a strongly cemented conglomerate with reworked boulders of MU-1a and similar faunal content; however distinctive cementation features can be observed in thin-section (Fig.6). The characteristics of the MU-1b deposit pointed to a relatively short sea-level oscillation that together with environmental conditions, promoted a fast early cementation, erosion and reworking of MU-1a, and eventual seaward accumulation of MU-1b.

At least three highstands characterize MIS 5e (Hearty et al., 2007; Rholing et al., 2019). In the Mediterranean coasts of Spain, oolitic sediments are always associated to the first, older, highstand and they usually accumulated as beach barrier– lagoon systems; the second highstand is represented by quartzous beach – dune systems; and the third highstand represents an important environmental change with high energy reddish conglomerates. The ages of these highstands have been stated by U-series between in 135 kyr and 117kyr and they are accompanied by changes in the environmental conditions (Hillaire-Marcel et al., 1986; Goy et al., 1993; Goy et al., 2006; Zazo et al., 2003; Bardají et al., 2009). Phreatic overgrowths on speleothemes from littoral caves in Mallorca point to two highstands during MIS 5e, with ages of 139 kyr and 114 kyr (Tuccimei et al., 2006). In Formentera, we have identified the same three highstands than in other peninsular and insular sites: a first oolitic beach (not outcropping above present sea level), second highstand (MU-1a), with reworked oolites, and the third highstand (MU-1b), a high energy deposit with boulders of reworked low-lying units, representing the increase in storminess recorded along the Spanish Mediterranean littoral at the end of MIS5e.

The third marine unit (MU-2) is a poorly cemented layer of reddish, *Glycymeris* -rich sandstone covering an erosional surface that onlaps the previous units, constitutes On the western part of the section, the upper surface of this layer is crisscrossed by polygonal cracks filled by a reddish terrestrial unit that contain also scattered shells of Glycymeris sp. (Figs. 5D and 8). This unit is interpreted as the upper foreshore / backshore, where small-scale sea-level changes promoted the occurrence of the polygonal cracks. The height of this unit (about 1.8m) and the sedimentological characteristics suggest a sea level very close to the present one during the time of deposition.

In Mallorca Island, Rose et al., (1999) describe a MIS 5a beach in Alcudia Bay at +3m amsl. Phreatic overgrowths in speleothems from littoral caves also form Mallorca, point to a short-lived highstand at +1,5-2m amsl also during MIS 5a (Tuccimei et al., 2006; Dorale et al., 2010). These data together with the fact there is not any reference to MIS5c deposits above present sea level in Baleares, and the sedimentary succession after this last evidence of sea level highstand, lead us to propose a MIS 5a age for this MU-2. This marine unit (MU-2) passes upwards to a reddish terrestrial unit TU-1) with scattered *Glycymeris* and other molluscs shells, as well as some angular carbonate fragments, that suggest a backshore environment in a descending sea level scenery, where coastal sediments are progressively replaced by an alluvial environment. The following sedimentary sequence, without any other evidence of marine environments and only alluvial and aeolian units outcropping, point to a MIS 5a age for this last marine unit.

5.2. MIS 5 – MIS 4 transition

The transition between MIS 5a and MIS 4 (GS23 to GS18) is marked in the Balearic Sea by an increased intensity of deep current (Torner et al., 2019) that is interpreted as the consequence of the weakening of the Atlantic Meridional Overturning Current (AMOC). This weakening lead to strong transport of dry and cold air masses by westerly winds which favoured evaporation and enhanced the Western Mediterranean Deep Water (WMDW) formation in the Gulf of Lion, and lower SST. Cooler SST may lead to more arid environments on land; however, this extreme aridity does not always accompany low SST (Hodge et al., 2008). Data from speleothems in Mallorca (Hodge et al., 2008; Fig. 15) show a growth hiatus during MIS5a but, in contrast, a continuous growing at the end of MIS5a and during MIS4, suggesting that cooler air temperatures maintained a critical moisture level in the Western Mediterranean. It’s noteworthy to highlight a rapid grow period at ca.77ka, coeval with GI20 and with a W-shaped (cooling-warm-cooling) SST, recorded in Balearic Sea (Core MD99-2343; Torner et al., 2019).

TU-1 in Formentera, although lacking a precise chronological data, show features pointing to a warm and humid climate, such as the high peak in magnetic susceptibility (Fig. 13), paleosol development and reddening (Fig. 8), that allow to tentatively correlate it to GI20.

Progressive aridity led to an increase in aeolian activity with a first development of an undulating deflation surface on TU-1, followed immediately upwards by large transversal dunes (72.8±7ka OSL), with abundant skeletal fragments and bioclasts, build by N-NW winds. Increased activity of the westerlies in the Gulf of Lion, revealed by the stronger WMDW recorded in Northern Menorca (Torner et al., 2019) could have been the cause of the prevailing N-NW winds in this area. It is worth to note that the abundant skeletal remains and bioclasts found into these dunes support a close descending sea level that followed the MIS5a highstand described for MU-2.

5.3. Climatic variability along MIS4 - MIS3

After the deposition of TU-2 dunes, the sea level lowstand during glacial MIS4 promoted the steep incision of former sedimentary units (Fig. 2). The following sedimentary terrestrial unit (TU-3) is characterized by a sudden change in driving winds. At the beginning of this period, large dunes with high sediment supply and relatively persistent northerly winds crossed the island. The high similarity between TU-2 dunes and older TU-3 dunes indicates similar driving mechanisms and environmental conditions: winds from the N-NW associated to increased activity of westerlies in the Gulf of Lion and aridity. These similarities, together with OSL age (54±5 ka BP) point to a late MIS4-beggining of MIS3 age for this unit.

Towards the top, prevailing winds rotated to the S-SW and barchanoid dunes accumulated following a remarkable diminution of sediment supply. Moister climate is evidenced by the dense bioturbation by plant roots. This sudden shift in wind direction and in vegetation cover, must be due to a change in regional climate. Warmer North Atlantic climate led to stronger AMOC, weaker westerlies blowing to the Gulf of Lion and therefore, less influence of northern winds in the island. A strong Azores anticyclone ruled the climate over Western Mediterranean, favouring thus the entry of southern winds coming from the warmer Algerian Basin. These climatic conditions and the OSL age (51±4 ka BP) allow to correlate these dunes with the warmer and wetter GI14-15 (Fig. 13).

A gently irregular erosion surface, with associated scree deposits, separates this unit from TU-4 suggesting that an intervening sudden arid event took place in between. Despite the intense bioturbation and weak cementation that favours weathering rubbing sedimentary structures, these TU-4 dunes seem to have grown under prevailing W-SW winds. The similarities found between this unit and younger TU-3 dunes, supported again by OSL ages (c. 53±5 ka BP) take us to give a MIS 3 age to this unit, most probably correlated to GI13-14 (Fig. 13)

Between 30ka and 50ka, North Atlantic climate displays very rapid warming and cooling episodes (Dansgaard et al., 1993; Rasmusen et al., 2002; NGRIP Members, 2004; Rasmussen et al., 2014) that impeded entering a full interglacial climate. Heinrich stadials (HS3, HS4 and HS5) punctuate the MIS3, driven by successive phases of AMOC weakening. However, in Western Mediterranean, these cold stages also show their own internal variability too. In the Balearic Sea, Sanchez Goñi et al. (2020) identify short-lived warming and wetting during HS4 and HS5, that contrast with the general cool and dry climate. Frigola et al., (2008) have also proposed a high variability pattern in the deep-water formation in Western Mediterranean along MIS3.

In our sedimentary sequence, climate variability is recorded by an alluvial /colluvial mass flow dominated sedimentary unit, punctuated by soil and calcrete development (TU-5). Quasi interglacial wetter climate, interpreted after the sedimentary characteristics and by the peaks in magnetics susceptibility, favoured dense vegetation cover avoiding dune development at least in this part of the island. OSL and TL ages support this chronological assumption (c.48±3, c.40±2 ka BP; 48,2 +8.1/-6.6 ka BP).

5.4. MIS2: The Last Glacial

Climate during MIS 2 (c. 11-28ka) is characterized worldwide by a general cold and arid climate, with the highest aridity in the Iberian Peninsula occurring during the Mystery Interval (MI 17.5 – 14.5 ka,), and the embedded H1 (16-17ka) (Moreno et al., 2012).

In our sequence, a sedimentary hiatus marks the first part MIS 2 with erosion and calcrete development characterizing the transit between TU-5 and TU-6 (Fig. 12). The age of this last unit (TU-6) is bracketed between 20±2 ka BP and 17+2.4/-2.2, very close to the extremely arid periods mentioned above, associated to GS2. However, although a cold and arid climate should be expected, this unit represents contrasting environmental conditions. A peak in magnetic susceptibility (Fig. 13), soil development, geochemical and mineralogical composition (Tables I, II & III), and above all, the phytolite content, all point to a humid and warm climate.

The explanation of this anomalous climate must lie in the recurrent abrupt climatic changes occurred during MIS2 (Fig. 15). The deglacial warming in the Alboran Sea was interrupted by severe cold shifts, coeval with H1 (Martrat et al., 2014), where multidecadal scale SST oscillations point to ca. +4ºC change in less than eight centuries. In the North Atlantic (Hodell et al., 2017) H1 is also characterized by two ice rafted debris layers (IRD) separated by a no-IRD layer, supporting a complex history of reduced AMOC by differential melting of the European and Laurentide Ice Sheets.

Greenland Stadial 2 (14.7 ka to 23.2 ka) is the most complex stadial described in the NGRIP records (Rasmussen et al., 2014), having been divided into GS-2.2, GS-2.1c, GS-2.1b and GS-2.1a, with the GS-2.1b (17.4 – 20.9 ka) being slightly warmer the others.

Given the chronological correlation between GS-2.1b and our sedimentary unit TU-6, we propose here that the slight recovery of AMOC circulation that may have caused the subtle warming during GS-2.1b could have been magnified in Western Mediterranean by a strong reduction of WMDW formation, by a similar mechanism than the one proposed by Sánchez-Goñi et al. (2020) to explain the warming events recorded in Western Mediterranean during HS4 and HS5.

The erosional flat surface on top of this unit implies an important gap in sedimentation, and a long-lasting extreme arid event which could have favoured wind deflation, desiccation, and cracking. TU-7 dunes mark the end of MIS2 with the phytolite content suggesting a progressive aridification.

6. CONCLUSIONS

The climatic variability in the North Atlantic along the Last Glacial Cycle (Termination II to Termination I) is recorded in Formentera Island (one of the westernmost Mediterranean islands) by changes in sedimentary style. Detailed geomorphological, geological and sedimentological study, supported by geochemical, soil and soil-morphology analyses, magnetic susceptibility, phytolite content and luminescence dating (TL, OSL) allowed to reconstruct the environmental evolution of this coastal setting. Three sea level highstands are recorded for MIS5e, and one more for MIS5a, which are congruent with sea level record from neighboring islands. Weakening of AMOC favor the enhancement of westerly winds in NW Europe, promoting the increase of northerly winds in Formentera, where different dune systems develop (MIS4 – beginning of MIS3). Stronger AMOC, weaken the influence of westerlies driving a change in prevailing winds in Formentera, where dunes start to grow under the influence of southerly winds and a moister climate. However, a change in sedimentary style during MIS3, with development of alluvial – colluvial units and intervening paleosols, witnesses the high climatic variability occurred during this stage in North Atlantic. After a long-lasting period of no deposition (end of MIS3 beginning of MIS2) a short interval of moister and warmer climate during GS-2.1b is followed by a progressive aridification, with dunes growing again under the influence of northerly winds at the end of MIS2.

Author contributions. **T. Bardají:** Term, Conceptualization, Investigation, Writing – Original draft, Editing. **E. Roquero:** Investigation (Paleosols, geochemistry), Resources, Writing – Review & Editing. **A. Cabero:** Conceptualization, Investigation (palaeontology, petrology), Resources, Writing – Original draft. **C. Zazo**: Term, Conceptualization, Investigation, Writing –Review & Editing, Supervision, Project Administration. **J.L. Goy:** Investigation, Project Administration, Funding acquisition. **C.J. Dabrio:** Investigation (sedimentology), Writing – Original draft, Review & Editing. **M.J. Machado**: Investigation (Phytolites). **J. Lario**: Investigation (Magnetic Susceptibility). **P.G. Silva:** Investigation (Tectonics). **A.M. Martínez-Graña:** Investigation (GIS)

Data availability. Other data than those included in the text can be obtained on request from the authors.

Declaration of competing interest. The authors declare that they have no known competing financial interests or personal relationships that could have appeared to influence the work reported in this paper.

REFERENCES

Albert R.M., Weiner S., 2001. Study of opal phytoliths in prehistoric ash layers using a quantitative approach. In: Meunier J, Coline F. eds. Phytoliths: applications in earth sciences and human history. Lisse, The Netherlands: Balkema, p: 251–266.

Alonso-Zarza, A. and Silva, P.G., 2002. Quaternary laminar calcretes with bee nests: evidences of small-scale climatic fluctuations, Eastern Canary Islands, Spain. Palaeogeography, Palaeoclimatology, Palaeoecology 178 (1-2), 119-135.

Bardaji, T., Dabrio, C.J., Goy, J.L., Somoza, L., Zazo, C. 1990. Pleistocene fan deltas in southeastern Iberian Peninsula: sedimentary controls and sea-level changes. In (A. Colella, D. B. Prior, Eds.): Coarse-grained Deltas. Special IAS Publication 10, 129-151.

Bardají, T.; Goy, J.L.; Zazo, C.; Hillaire-Marcel,Cl.; Dabrio, C.J.; Cabero, A.; Ghaleb, B.; Silva,P.G., 2009. Sea level and climate changes during OIS 5 in Western Mediterranean (Spain). Geomorphology 104, 22-37

Bardají, T., Cabero, A., Lario, J. Dabrio, C.J., Zazo, C., Goy, J.L., Silva, P.G., Roquero, E. 2013. Evidencias morfosedimentarias de descensos rápidos del nivel del mar durante el MIS 5e en el Mediterráneo español. In (Baena et al., Eds.). El Cuaternario Ibérico: Investigación en el Siglo XXI.

Bond, G., Heinrich, H., Broecker, W., Labeyrie, l., McManus, J., Andrews, J., Huon, S., Jantschik, R., Clasen, S., Simet, C., Tedesco, K., Klas, M., Bonani, G., Ivy, S., 1992. Evidence for massive discharges of icebergs into the North Atlantic Ocean during the last glacial period. Nature 360, 245-249.

Bond, G., Broecker, W., Johnson, S., McManus, J., Labeyrie, l., Jouzel, J., Bonani, G., 1993. Correlations between climate records from North Atlantic sediments and Green-land ice. Nature, 365, 143-147.

Bond, G., Showers, W., Cheseby, M., Lotti, R. Almasi, P. deMenocal P., Priore, P., Cullen H., Hajdas, l. Bonani, G., 1997. A pervasive millenial-scale cycle in North Atlantic Holocene and glacial climates. Science 278, 1257-1266.

Bullock, P., Fedoroff, N., Jongerius, A., Stoops, G., Tursina, T., 1985. Handbook for soil thin section description. Wayne Research Publications, U.K., 150pp.

Butzer and Cuerda, 1962. Coastal stratigraphy of suother Mallorca and its implications for the Pleistocene chronology

Cabra,P., Garcia de Domingo, A., Diaz de Neira, J.A., Gil, J. 2009. Mapa geológico de España, 2º serie, Sc:125.000, Formentera (824 IV/825 III).IGME

Cacho, I., Grimalt, J.O., Pelejero, C., Canals, M., Sierro, F.J., Flores, J.A., Shackleton, N. 1999. Dansgaard-Oeschger and Heinrich event imprints in Alboran Sea paleotemperatures. Paleoceanography 14(6), 698-705.
Clemmensen, L.B., Lisborg, T., Fornós, J.J., Bromley, R., 2001. Cliff-front Aeolian and colluvial deposits, Mallorca, Western Mediterranean: a record of climatic and environmental change during the last glacial period. Bulletin of the Geological Society of Denmark 48, 217–232.
Costa, M., Cuerda, J., Roselló, V.M., 1985. Formentera i els Estanys. Panorama geoecològic des del Quaternari. Cuadernos de Geografía (Dep. Geog. Univ. Valencia) 37, 75-96.
Cuerda, J. (1984). A contribution to the knowledge of Pleistocene coastal profiles in the Pityusic Islands. Publ. In Monographiae biologicae, 52 Biogeography of the Pityusic Islands. The Hague-Boston-Lancaster, 105-118.
Cuerda, J. (1989): Los tiempos Cuaternarios en Baleares. Dir. Gral. Cultura, Conselleria de Cultura, Educació i Esports. Govern Balear, Mallorca. 305 pp.
Dabrio, C.J., Zazo, C., Cabero, A., Goy, J.L., Bardají, T., Hillaire-Marcel, C., González-Delgado, J.A., Lario, J., Silva, P., Borja, F., García-Blázquez, A.M., 2011. Millennial/submillennial-scale sea-level fluctuations in western Mediterranean during the second highstand of MIS 5e. Quaternary Science Reviews 30, 335–346.
Dansgaard, W., Clausen, H.B., Gundestrup, N., Hammer, C.U., Johnsen, S.F., Kristindottir, P.M., Reeh, N., 1982. A New Greenland Deep Ice Core. Science 218, 1273-1277.
Dansgaard, W., Johnsen, S.J., Clausen, H.B., Dahl-Jensen, D., Gundestrup, N.S., Hammer, C.U., Hvidberg, C.S., Steffense, J.P., Sveinbjörnsdottir, A.E., Jouzel, J., Bond, G., 1993. Evidence for general instability of past climate from a 250-kyr ice-core record. Nature 364, 218-
Del Valle, L., Pomar, F., Fornós, J.J., Gómez-Pujol, L., Timar-Gabor, A., 2018. Lower to Late Pleistocene coastal deposits of Eivissa (Western Mediterranean): Chronology and evolution. VII Jornades de Medi Ambient de les Illes Balears (Mallorca, 2018), Abstract Volume, 27-30.
Del Valle, L., Fornós, J.J., Pomar, F., Pons, G.X., Timar-Gabor, A., 2020. Aeolian-alluvial interactions at Formentera (Balearic Islands, Western Mediterranean): The late Pleistocene Evolution of a Coastal system. Quaternary International 566-567, 271–283.
Del Valle, L., Timar-Gabor, A., Pomar, F., Pons, G.X., Fornós, J.J., 2021. Millennialscale climate variability recorded in Late Pleistocene coastal deposits of Formentera Island (Balearic Archipelago, Western Mediterranean). Quaternary International (in press, available online)
Dorale, J.A.; Onac, B.P.; Fornós, J.J.; Ginés, J.; Ginés, A.; Tuccimei, P. & Peate, D.W., 2010. Sea level 81,000 years ago in Mallorca. Science 327, 860-863.
Fiol, Ll., Fornós, J.J., Gelabert, B., Guijarro, J.A., 2005. Dust rains in Mallorca (Western Mediterranean): Their occurrence and role in some recent geological processes. Catena 63, 64-84.
Fletcher, W.J. and Sánchez-Goñi, M.F., 2008. Orbital- and sub-orbital-scale climate impacts on vegetation of the western Mediterranean basin over the last 48,000 yr. Quaternary Research 70, 451-464.
Flügel, E., 2010. Microfacies of Carbonate Rocks: Analysis, Interpretation and Application. Springer, Berlin, Heidelberg. 984pp.
Fornós, J.J., Clemmensen, L.B., Gómez-Pujol, L., Murria, A.S. (2008). El Pleistoceno superior de Mallorca (Mediterráneo occidental): nuevas dataciones por luminiscencia (OSL) en los depósitos eólicos carbonatados y sus implicaciones paleoambientales. Geotemas, 10, 739-742.
Frigola, J., Moreno, A., Cacho, I., Canals, M., Sierro, F.J., Flores, J.A., Grimalt, J.O., Hodell, D.A., Curtis, J.H. 2007. Holocene climate variability in the western Mediterranean region from a deep-water sediment record. Paleoceanography 22, PA2209.
Frigola, J., Moreno, A., Cacho, I., Canals, M., Sierro, F.J., Flores, J.A., Grimalt, J.O. 2008. Evidence of abrupt changes in Western Mediterranean Deep-Water circulation during the last 50kyr: a high-resolution marine record from the Balearic Sea. Quaternary International 181, 88-104.

Gàsser, Z., 1998. Nota paleontològica sobre el jaciment quaternari marí d'Es Copinar (Formentera, Illes Pitiüses, Mediterrània occidental). Bolletí de la Societat d'Història Natural de les Balears 41, 153-157.

Gàsser, Z., 2002. Jaciments paleontològics marins del Miocè I Quarternari d'es Ram (Formentera, Illes 676 Pitiüses). Bolletí de la Societat d'Història Natural de les Balears 45, 87-92.

Gàsser, Z. and Ferrer, J.A.,1997. Nous Jaciements paleontològics del Miocè i Quaternari de Formentera (IllesPitiüses, Mediterrània Occidental). Boll. Soc. d'Hist. Nat. Balears 40, 91-101.

Gill, R. 1997. Modern Analytical Geochemistry: An Introduction to Quantitative Chemical Analysis Techniques for Earth, Environmental and Materials Scientists (Longman Geochemistry Series)Taylor & Francis LTD, U.K., 342pp.

Ginés, J.; Fornós, J.J. & Ginés, A. (2005): Els espeleotemes freàtics del Quaternari de Mallorca: aspectes morfològics, mineralògics i cristal·logràfics. In: Sanjaume, E. & Mateu, J.F. (eds.) Geomorfologia litoral i Quaternari. Homenatge al professor Vicenç M. Rosselló i Verger. Universitat de València, 151-165.

Ginés, J., Ginés, A., Fornós, J.J., Tuccimei, P., Onac, B.O., Gràcia, F., 2012. Phreatic Overgrowths on Speleothems (POS) from Mallorca, Spain: Updating forty years of research. In Ginés, A., Ginés, J., Gómez-Pujol, L., Onac, B.P. & Fornós, J.J. (eds.). Mallorca: A Mediterranean Benchmark for Quaternary Studies. Mon. Soc. Hist. Nat. Balears 18, 111-146.

González-Hernández, F.M., Goy, J.L., Zazo, C., Silva, P.G., 2001. Actividad eólica - cambios del nivel del mar durante los últimos 170.000 años (litoral de Mallorca, Islas Baleares). Cuaternario y Geomorfología 15(3-4), 67-75

Goy, J.L., Zazo, C., Bardají, T., Somoza, L., Causse, Ch., Hillaire-Marcel, C.I., 1993. Eléments d'une chronostratigraphie du Tyrrhénien des régions d'Alicante-Murcie, Sud-Est de l'Espagne. Geodinamica Acta 6, 103–119.

Goy, J.L., Zazo, C., Cuerda, J., 1997. Evolución de las áreas margino-litorales de la costa de Mallorca (I. Baleares) durante el último y presenta interglacials: nivel del mar holoceno y clima. Boletín Geológico y Minero 108, 455–463.

Goy, J.L., Hillaire-Marcel, C.I., Zazo, C., Ghaleb, B., Dabrio, C.J., González-Delgado, J.A., Bardají, T., Civis, J., Preda, M., Yébenes, A., Forte, A.M., 2006. Further evidence for a relatively high sea level during the Penultimate Interglacial, open system U-series ages from La Marina (Alicante, East Spain). Geodinamica Acta 19, 409– 426.

Goy, J.L., Zazo, C., Cabero, A., Mercier, N., Bardají, T., Soler, V., Silva, P.G., Dabrio, C.J. (2007). Inestabilidad climática y del nivel del mar durante el óptimo del Ultimo Interglacial (Eivissa-Formentera). En: Lario, J.&Silva,P.G. (eds.). Contribuciones al Estudio del Periodo Cuaternario, Ávila, 179-180.

Goy, J.L., Zazo, C., Dabrio, C.J., Cabero, A., Lario, J., Roquero, E., Mercier, N., Soler, V. (2010). Marine and terrestrial environment relationships in coastal áreas during Late Pleistocene (Formentera, Balearic Isalnds). Abstract Volume, International *Workshop on "Decoding the Last Intergalcial in Western Mediterranean",* Cerdeña (Italia), Octubre-2010, pp.27

Hearty, P.J., 1987. New data on the Pleistocene of Mallorca. Quaternary Science Reviews 6, 254–257.

Hearty, P.J., Hollin, J.T., Neumann, A.C., O'Leary, M.J., McCulloch, M., 2007. Global sealevel fluctuations during the Last Interglaciation (MIS 5e). Quaternary Science Reviews 26, 2090–2112.

Heinrich, H., 1988. Origin and consequences of cyclic ice rafting in the Northeast Atlantic Ocean during the past 130,000 years. Quaternary Research 29(2), 142-152.

Heller, F., Liu, X.M., Liu, T.S., Xu, T., 1991. Magnetic susceptibility of loess in China. Earth and Planetary Science Letters 103, 301–310.

Hillaire-Marcel, C., Carro, O., Causse, C., Goy, J.L., Zazo, C., 1986. Th/U dating of Strombus bubonius bearing marine terraces in southeastern Spain. Geology 14, 613–616.

Hillaire-Marcel, C., Gariépy, C., Ghaleb, B., Goy, J.L., Zazo, C., Cuerda, J., 1996. U-series measurements in Tyrrhenian deposits from Mallorca. further evidence for two last-interglacial high sea levels in the Balearic Islands. Quaternary Science Review 15, 53-62

Hodell, D.A., Nicholl, J.A., Bontognali, T.R., Danino, S., Dorador, J., Downdeswell, J.A., Einsle, J., Kuhlmann, H., Martrat, B., Mleneck-Vautravers, M.J., Rodríguez-Tovar, F.J., Röhl, U., 2016. Anatomy of Heinrich Layer 1 and its role in the last deglaciation, Paleoceanography, 32, 284–303.

Hodge, E.J., Richards, D.A., Smart, P.L., Ginés, A., Mattey, D.P., 2008. Sub-millennial climate shifts in the western Mediterranean during the last glacial period recorded in a speleothem from Mallorca, Spain. Journal of Quaternary Science 23 (8), 713-718

Hoogakker, B.A.A., Rothwell, R.G., Rohling, E.J., Paterne, M., Stow D.A.V., Herrle J.O., Clayton T., 2004. Variations in terrigenous dilution in western Mediterranean Sea pelagic sediments in response to climate change during the last glacial cycle. Marine Geology 211, 21-43.

Hughes, P.D., Gibbard, P.L., Ehlers, J. 2013. Timing of glaciation during the last glacial cycle: evaluating the concept of a global ‘Last Glacial Maximum’. Earth-Science Reviews 125, 171-198.

Kukla, G., Melice, J.L., Gavin, J., Xiao, J.L., 1990. Magnetic susceptibility of Chinese loess. Transactions of the Royal Society of Edinburgh (Earth Sciences) 81, 263–288.

Lewis, D.W. and McConchie, D., 1994. Analytical Sedimentology, Chapman & Hall, New York, London, 197pp.

Locarnini, R. A., A. V. Mishonov, J. I. Antonov, T. P. Boyer, H. E. Garcia, O. K. Baranova, M. M. Zweng, C. R. Paver, J. R. Reagan, D. R. Johnson, M. Hamilton, D. Seidov, 2013. World Ocean Atlas 2013, Volume 1: Temperature. S. Levitus, Ed.; A. Mishonov, Technical Ed.; NOAA Atlas NESDIS 73, 40 pp.

Macklin, M.G., Fuller, I.C., Lewin, J., Maas, G.S., Passmore, D.G., Rose, J., Woodward, J.C., Black, S.,Hamnli, R.H.B., Rowan, J.S., 2002. Correlation of fluvial sequences in the Mediterranean basin over the last 200 ka and their relationship to climate change. Quaternary Science Reviews 21, 1633-1641.

Madella M., Powers-Jones A.H., Jones M.K. 1998. A Simple Method of Extraction of Opal Phytoliths from Sediments Using a Non-Toxic Heavy Liquid. *Journal of Archaeological Science*, 25(8):801–803

Madella M., Alexandre, A., Ball, T. 2005. International Code for Phytolith Nomenclature 1.0. *Annals of Botany*, 96: 253–260.

Maher, B.A., 1998. Magnetic properties of modern soils and Quaternary loessic paleosols: paleoclimatic implications. Paleogeography, Paleoclimatology, Paleoecology, 137, 25–54.

Martínez-Ruíz, F., Kastner, M., Gallego-Torres, D., Rodrigo-Gámiz, M., Nieto-Moreno, V., Ortega-Huertas, M., 2015. Paleoclimate and paleoceanography over the past 20,000 yr in the Mediterranean Sea Basins as indicated by sediment elemental proxies. Quaternary Science Reviews 107, 25-46.

Martrat, B., Grimalt, J.O., López-Martínez, C., Cacho, I., Sierro, F.J., Flores, J.A., Zahn, R., Canals, M., Curtis, J.H., Modell, D.A., 2004. Abrupt temperature changes in the Western Mediterranean over the past 250,000 years. Science 306, 1762–1765.

Martrat, B., Jimenez-Amat, P., Zahn, R., Grimalt, J.O., 2014. Similarities and dissimilarities between the last two deglaciations and interglaciations in the North Atlantic region. Quaternary Science Reviews 99, 122-134.

Maslin, M., Seidov, D., Lowe, J. (2001) Synthesis of the natures and causes of rapid climate transitions during the Quaternary. In: The Oceans and rapid climate change: Past, Present and Future, AGU Geophysical Monograph 126, 9-52.

McManus, J.F., Oppo, D.W., Gullen, J.L., 1999. A 0.5 million year record of millennial-scale climate variability in the North Atlantic. Science 283, 971-975.

McManus, J.F., Francois, R., Gherardi, J.M., Keigwin, L.D.,Brown-Leger, S, 2004. Collapse and rapid resumption of Atlantic meridional circulation linked to deglacial climate changes. Nature 428, 834-837.
Millot, C., 1999. Circulation in Western Mediterranean. Journal of Marine Systems 20, 423–442.
Millot, C., Taupier-Letage, I., 2005. Circulation in the Mediterranean Sea. In The Handbook of Environmental Chemistry, Springer-Verlag, Berlin, pp. 29–66.
Moreno, A., Cacho, I., Canals, M., Sánchez-Goñi, M.F., Grimalt, J.O., Sierro, F.J. (2007) Land-Sea intercations from a high frequency multi-proxy study of the last 50.000yr (Alboran Sea, Western Mediterranean). Quaternary International 167-168, 288-289.
Moreno, A., Stoll, H., Jiménez-Sánchez, M., Cacho, I., Valero-Garcés, B., Ito, E., Lawrence Edwards, R. 2010. A speleotheme record of glacial (25-11.6 kyr BP) rapid climatic changes from northern Iberian Peninsula. Global and Planetary Change 71, 218-231.
Moreno, A., González-Sampériz, P., Morellón, M., Valero-Garcés, B.L., Fletcher, W.J. (2012). Northern Iberian abrupt climate change dynamics during the last glacial cycle: A view from lacustrine sediments. *Quaternary Science Reviews*, 36, 139-153.
Muhs, D.R., Budahn, J., Avila, A., Skipp, G., Freeman, J., Patterson, D., 2010. Geochemical evidence for African dust additions to Quaternary soils on the island of Mallorca, Spain and implications for the genesis of Red Mediterranean soils. Quaternary Science Reviews 29, 2518–2543.
Muhs, D.R., Simmons, K.R., Meco, J., Porat, N., 2015. Uranium-series ages of fossil corals from Mallorca, Spain: The “Neotyrrhenian” high stand of the Mediterranean Sea revisited. Palaeogeography, Palaeoclimatology, Palaeoecology 438, 408–424.
Murray, R.W., Miller, D.J., and Kryc, K.A. 2000. Analysis of major and trace elements in rocks, sediments, and interstitial waters by inductively coupled plasma–atomic emission spectrometry (ICP-AES). ODP Technical Note 29 [Online].
NGRIP Members, 2004. High resolution climate record of the Northern Hemisphere back to the last interglacial period. Nature 431, 147–151.
Nielsen, K.A., Clemmensen, L.B., Fornós, J.J., 2004. Middle Pleistocene magnetostratigraphy and susceptibility stratigraphy: data from a carbonate aeolian system, Mallorca, Western Mediterranean. Quaternary Science Review 23,1733-1756.
Onac, B.P., Ginés, A., Ginés, J., Fornós, J.J., Dorale, J.A., 2012. Late Quaternary Sea-level History: a Speleothem Perspective. In: Ginés, A., Ginés, J., Gómez-Pujol, L., Onac, B.P. & Fornós, J.J. (eds.). 2012. Mallorca: A Mediterranean Benchmark for Quaternary Studies. Mon. Soc. Hist. Nat. Balears 18, 147-162.
Parr J.F., Lentfer C.J., Boyd W.E. 2001. A comparative analysis of wet and dry ashing techniques for the extraction of phytoliths from plant material. Journal of Archaeological Science 28, 875-886.
Pomar, F., del Valle, L., Fornós, J.J., Gómez-Pujol, Ll., 2018. Late Pleistocene dune-sourced alluvial fans in coastal settings: Sedimentary facies and related processes (Mallorca, Western Mediterranean). Sedimentary Geology 367, 48-68.
Rasmunsen, T.L., Thomsen, E., Troelstra, S.R., Kuijpers, A., Prins, M.A., 2002. Millennial-scale glacial variability versus Holocene stability: changes in planktic and benthic foraminifera faunas and ocean circulation in the North Atlantic during the last 60 000 years. Marine Micropaleontology 47, 143-176.
Rasmussen, S.O., Bigler, M., Blockley, S.P., Blunier, T., Buchardt, S.L., Clausen, H.B., Cvijanovic, I., Dahl-Jensen, D., Johnsen, S.J., Fischer, H., Gkinis, V., Guillevic, M., Hoek, W.Z., Lowe, J.J., Pedro, J.B., Popp, T., Seierstad, I.K., Steffensen, J.P., Svensson, A.M., Vallelonga, P., Vinther, b.m., Walker, M.J.C., Wheatley, J.J., Winstrup, M. 2014. A stratigraphic framework for abrupt climatic changes during the Last Glacial period based on three synchronized Greenland ice-core records: refining and extending the INTIMATE event stratigraphy. Quaternary Science Reviews 106, 14-28

Rholing, E.J., Hibbert, F.D., Grant, K.M., Galaasen, E.V., Irvali, N., Kleiven, H.F., Marino, G., Ninnemann, U., Roberts, A.P., Rosenthal, Y., Schulz, H., Williams, F.H., Yu, J., 2019. Asynchronous Antarctic and Greenland ice-volume contributions to the last interglacial sea-level highstand. Nature Communications 10:5040.

Roep, T.B., Dabrio, C.J., Fortuin, A.R., Polo, M.D., 1998. Late highstand patterns of shifting and stepping coastal barriers and washover-fans (Late-Messinian, Sorbas Basin, SE Spain). Sedimentary Geology 116, 27-56.

Rose, J., Meng, X., Watson, C. 1999. Paleoclimate and palaeoenvironmental responses in the western Mediterranean over the last 140ka: evidence from Mallorca, Spain. Journal of the Geological Society of London 156, 435-448.

Sánchez-Goñi, M.F., Loutre, M.F., Crucifix, M., Peyron, O., Santos, L., Duprat, J., Malaiz_e, B., Turon, J.L., Peypouquet, J.P., 2005. Increasing vegetation and climate gradient in western Europe over the last glacial inception (122-110 ka): datamodel comparison. Earth Planetary Sciences Letters 231, 111-130.

Sánchez-Goñi, M.F., Fourcade, T., Salonen, S., Lesven, J., Frigola, J., Swingedouw, D., Sierro, F.J., 2020. Muted cooling and drying of NW Mediterranean in response to the strongest last glacial North American ice surges. GSA Bulletin

Sarnthein, M., Stattegger, K., Dreger, D., Erlenkeuser, H., Grootes, P., Haut, B., Jung, S., Kiefer, T., Kuhnt, W., Pflaumann, U., Schäfer-Neth, C., Schulz, H., Schulz, M., Seidov, D., Simstich, J., van Kreveld, S., Vogelsang, E., Völker, A., Weinelt, M., 2000. Fundamental Modes and Abrupt Changes in North Atlantic Circulation and Climate over the last 60 ky – Concepts, Reconstruction and Numerical Modeling. In: P. Schäfer,W. Ritzrau, M. Schlüter, and J. Thiede (Eds): The Northern North Atlantic: A Changing Environment, Springer, Berlin, pp. 365–410,

Servera, J. & Grimalt, M. (1994). Los sistemas dunares de las Islas de Formentera y de s'Espalamador. En: Geomorfología en España (J. Arnaéz, J.M. García Ruiz & A. Gómez Villar, eds.). Sociedad Española de Geomorfología. Logroño, 1, 405 – 418

Torner, J., Cacho, I., Moreno, A., Sierro, F.J., Martrat, B., Todríguez-Lázar, J., Frigola, J., Arnau, P., Belmonte, A., Hellstrom, J., Cheng, H., Lawrences Edwards, R., Stoll, H. 2019. Ocean-atmosphere interconnections from the last interglacial to the early glacial: An integration of marine and cave records in the Iberian region. Quaternary Science Reviews 226, 106037.

Tuccimei, P., Ginés, J., Delitala, M.C., Ginés, A., Gràcia, F., Fornós, J.J., Taddeucci, A., 2006.High precision U-series data from phreatic overgrowths on speleothems. Zeitschrift fur Geomorphologie 50, 1–21.

Tuccimei, P., Onac, B.P-, Dorale, J.A., Ginés, J., Fornós, J.J., Ginés, A., Spada, G., Ruggieri, G., Mucedda, M., 2012. Decoding last interglacial sea-level variations in the western Mediterranean using speleothem encrustations from coastal caves in Mallorca and Sardinia: A field data – model comparison. Quaternary International 262, 56-64.

Vesica, P.L., Tuccimei, P., Turi, B., Fornós, J.J., Ginés, A., Ginés, J., 2000. Late Pleistocene Paleoclimates and sea-level change in the Mediterranean as inferred from stable isotopes and U-series studies of overgrowths on speleothems. Quaternary Science Reviews 19, 865–879.

Vicens, D., Gràcia, F., Cuerda, J., 1992. El Quaternari marí del Torrent Fondo (Formentera, Illes Pitiuses). Boll. Soc. Hist. Nat. Balears 35, 61-66.

Wanless, H.R., Tedesco, L.P., 1993. Comparison of oolitic sand bodies generated by tidal vs. wind-wave agitation. In: Keith, B.D., Zuppman, C.W. (Eds.), Mississippian oolites and modern analogs. AAPG Studies in Geology 35, 199–225.

Zazo, C., Goy, J.L., Dabrio, C.J., Bardají, T., Hillaire-Marcel, C., Ghaleb, B., González-Delgado, A., Soler, V., 2003. Pleistocene raised marine terraces of the Spanish Mediterranean and Atlantic coasts: records of coastal uplift, sea-level highstands and climate changes. Marine Geology 194, 103–133.

Zazo, C., Dabrio, C.J., Goy, J.L., Lario, J., Cabero, A., Silva, P.G., Bardají, T., Mercier, N., Borja, F., Roquero, E., 2008. The coastal archives of the last 15 ka in the Atlantic-Mediterranean Spanish linkage area: sea level and climate changes. Quaternary International 181, 72-87.

Zhang, X., Knorr, G., Lohmann, G., Barkeer, S., 2017. Abrupt North Atlantic circulation changes in response to gradual CO_2 forcing in a glacial climate state. Nature Geoscience 10, 518-523.

Zheng, H.B., Oldfield, F., Wintle, A.G., Robinson, S.G., Wang, J.T., 1990. The magnetic properties of particle-sized samples from the Luochuan loess section: evidence for pedogenesis. Physics of the Earth and Planetary Interiors 68, 250–258.

Zweng, M. M, J. R. Reagan, J. I. Antonov, R. A. Locarnini, A. V. Mishonov, T. P. Boyer, H. E. Garcia, O.K. Baranova, D.R. Johnson, D. Seidov, M.M. Biddle, 2013. World Ocean Atlas 2013, Volume 2: Salinity

Figure captions

Figure 1. Location of studied area within the Western Mediterranean framework. A) Main currents based on Millot (1999); Average Sea Surface Temperature data from Medspiration Project (ESA's Sentinel-3 mission); B) Location of Formentera Island within the Balearic Islands' archipelago; dashed blue line roughly outline the Balearic promontory.

Figure 2. Geological and geomorphological sketch of Formentera Island.

Figure 3. A) Synthetic section of the sedimentary sequence along Es Copinyar – Caló des Morts with location of Terrestrial (TU) and Marine Units (MU) described in text, TSL-OL (orange circles) and magnetic susceptibility samples (green circles); B) Part of the sequence outcropping at Caló des Morts.

Figure 4. Synthetic stratigraphic column of the sedimentary sequence along Es Copinyar – Caló des morts. Same terrestrial (TU) and marine (MU) units than in Fig. 3

Figure 5. MIS 5 marine units. A) Marine Unit 1b (MU-1b) off-lapping a small cliff carved into Marine Unit 1a (MU1a); B) Close view of MU-1b filling cracks and potholes carved into MU-1a, with reddish clay matrix and reworked boulders and cobbles of MU-1a; C) *Strombus bubonius* into MU-1a; D) Upper part of MU-2, with abundant *Glycymeris sp* overlapped by reddish terrestrial units 1 and 2 (TU-1, TU-2),

Figure 6. Thin sections of marine units. A) B) y C) corresponds to MU-1a; D) MU-1bB: Bioclast; RF: Rock fragment; ORF: Oolithic rock fragment; Oo: oolithe; O-Ag: Oolithic agregates; AC: aragonite coating; Cc: Crustacean microcoprolite (Palaxius?); Pf: planktonic foraminifera; Raf: Red algae fragment; m: micritic cement; sp: sparite cement.

Figure 7. Accumulation of *Glycymeris* sp. shells on the upper foreshore (A) and backshore (B) at Es Copinyar present beach.

Figure 8. Terrestrial Unit 1 (TU-1) developed over MU-2, and paleosol horizons described in text. Properties of paleosol in Table I.

Figure 9. Terrestrial Unit TU-3 adjusting its development to the erosional surface carved intro previous sedimentary units. A) TU3-a and TU-3b overlapping TU 1; B) TU-3 reaching down to MU-1.

Figure 10. Main characteristics of terrestrial units outcropping along Es Copinyar – Caló des Morts cliff. A) Migration of different sets of TU-3 in opposite directions; B) Abundant clasts in scree deposits developed in the topographically lower parts of unit TU-4; C) Root bioturbation in upper part of TU-4; D) Superposition of TU-7 over TU-6; Flat deflation surface between TU-6 and TU-7; F) Detail of surface between TU-6 and TU-7 showing a thin calcareous accumulation and retraction cracks.

Figure 11. Terrestrial Unit 5 (TU-5) displaying several pedo-sedimentary cycles clearly distinguishable by vertical distribution of some paleosol properties (see Table I).

Figure 12. Terrestrial Unit 6 (TU-6) with indication of soil horizons described in text (see properties in Table I).

Figure 13. Correlation of magnetic susceptibility results with the synthetic stratigraphic column. Green circles mark the location of magnetic susceptibility samples; a…z, α, β,γ corresponds to sample sites.

Figure 14. Fossil phytolith content and associated vegetation cover types along terrestrial units of Es Copinyar sequence (a…z, α, β,γ corresponds to sample sites).

Fig. 15. Chronology of events from the studied sequence and correlation with data from other authors. MIS boundaries from Lisiecki & Raymo (2005). H1,…H6: Heinrich events. a) $\delta^{18}O$ (violet line)

and temperature (orange dashed line) from the NGRIP ice core, (NGRIP members, 2004; Kindler et al., 2014). Age of Greenland Interstadials (GI) and Stadials (GS) from Rasmunsen et al. (2014); b) Data from stalactite in Mallorca, (Hodge et al., 2008); c) Fluvial aggradation phases in Mallorca (Torrente d’es Coco; Macklin & Lewin, 2008); d) SST from Alboran Sea (Martrat et al., 2014); e) Sea level curve for MIS5 in Mallorca (Dorale et al., 2010); f) Results of this work. G.v.: *Glycimeris violacences*; S.b.: *Strombus bubonius* (=*Persististrimbus latus*); m&w: moist and warm.

Table I. Properties of soils developed in Terrestrial Units 1, 5 and 6

Table II. DRX results of samples from Caló des Mort sequence (location of sample sites in Figs. 3 and 4).

Table III. Geochemical results of samples (major components) from Caló des Mort sequence (location of sample sites in Figs. 3 and 4)

Figure 1

Click here to download Figure Figure 1.png

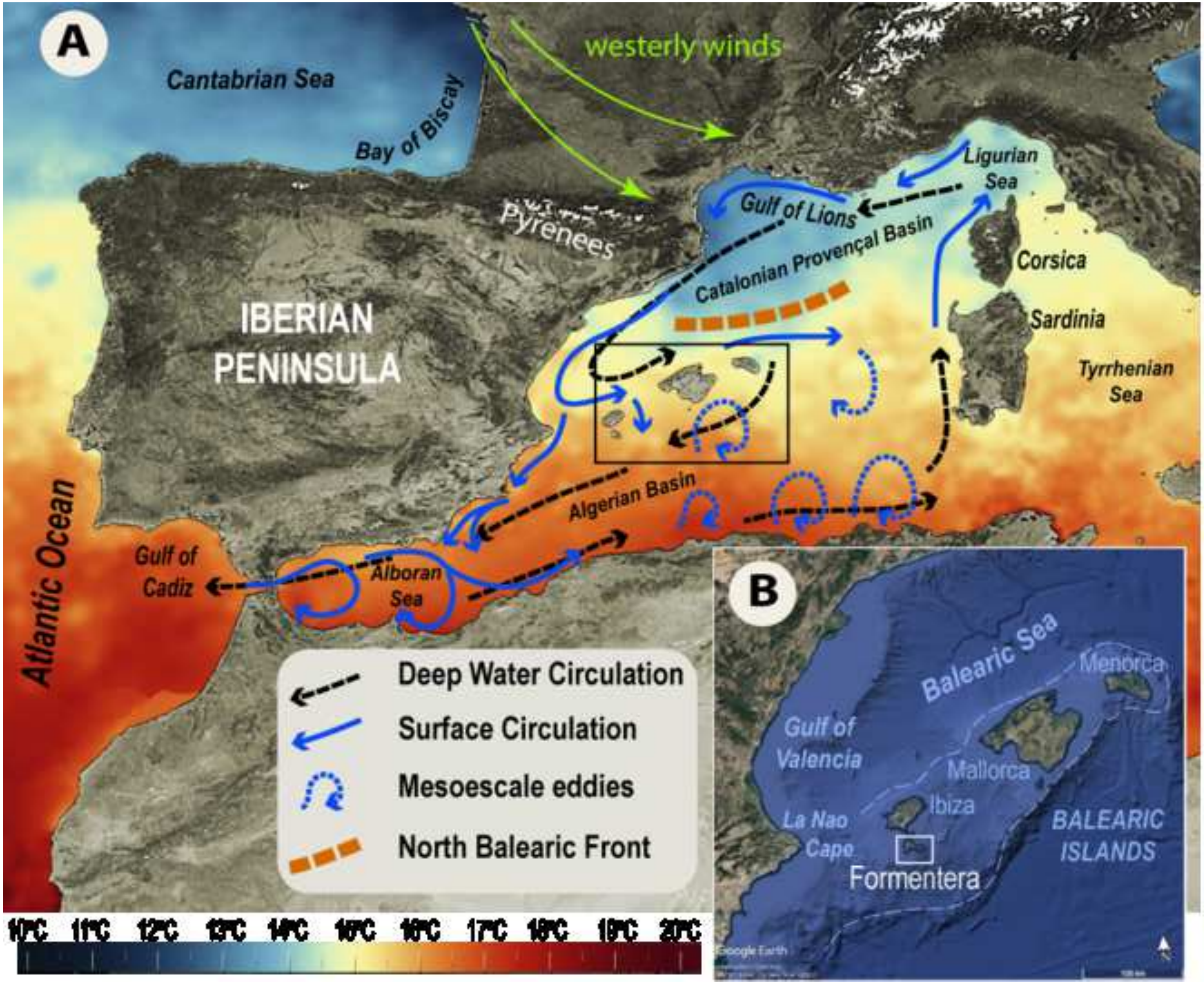

Figure 2 Click here to download Figure Figure 2-iMac.png

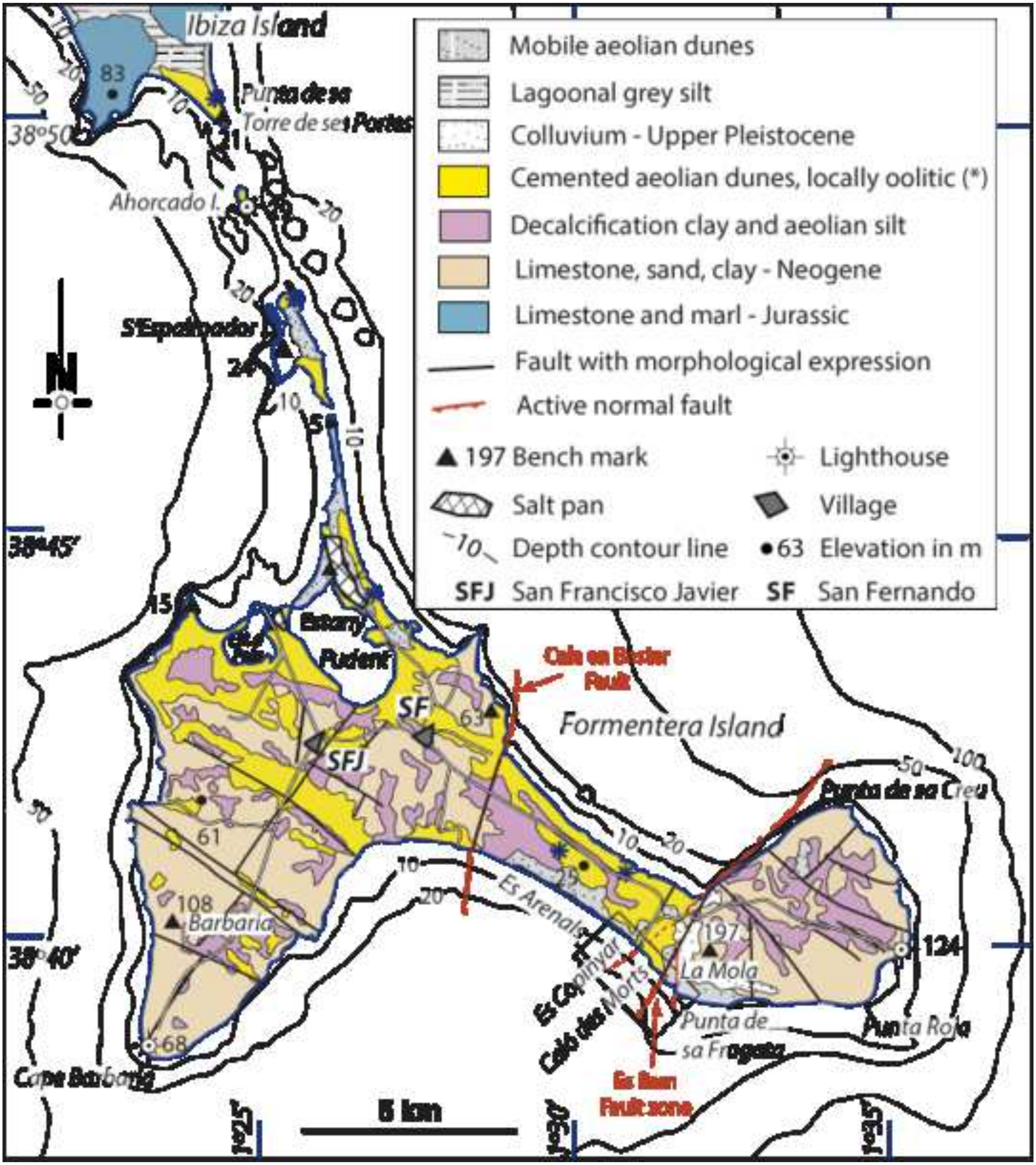

Figure 3

Click here to download Figure Figure 3.png

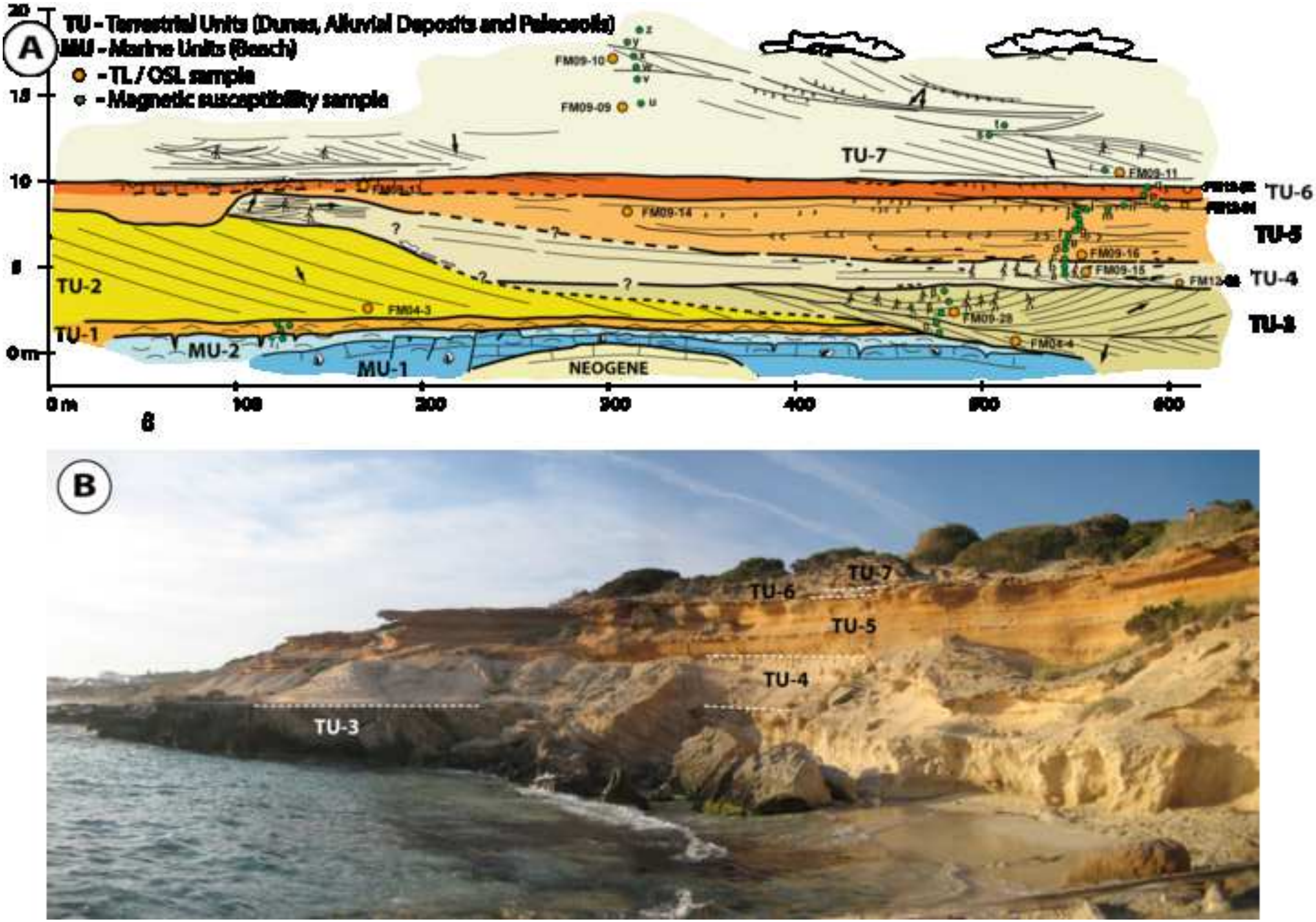

Figure 4

Click here to download Figure Figure 4.png

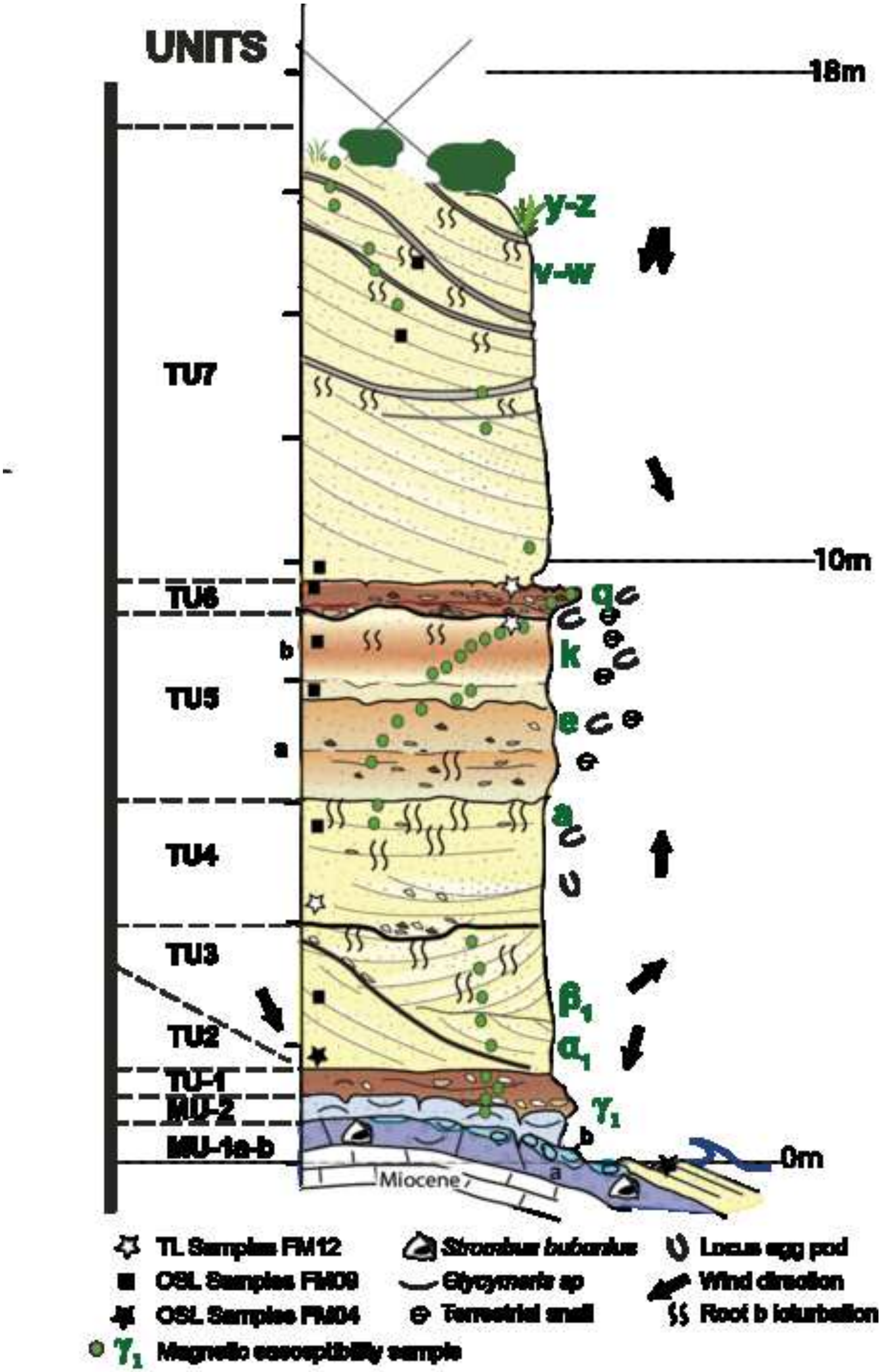

Figure 5 Click here to download Figure Figure 5.png

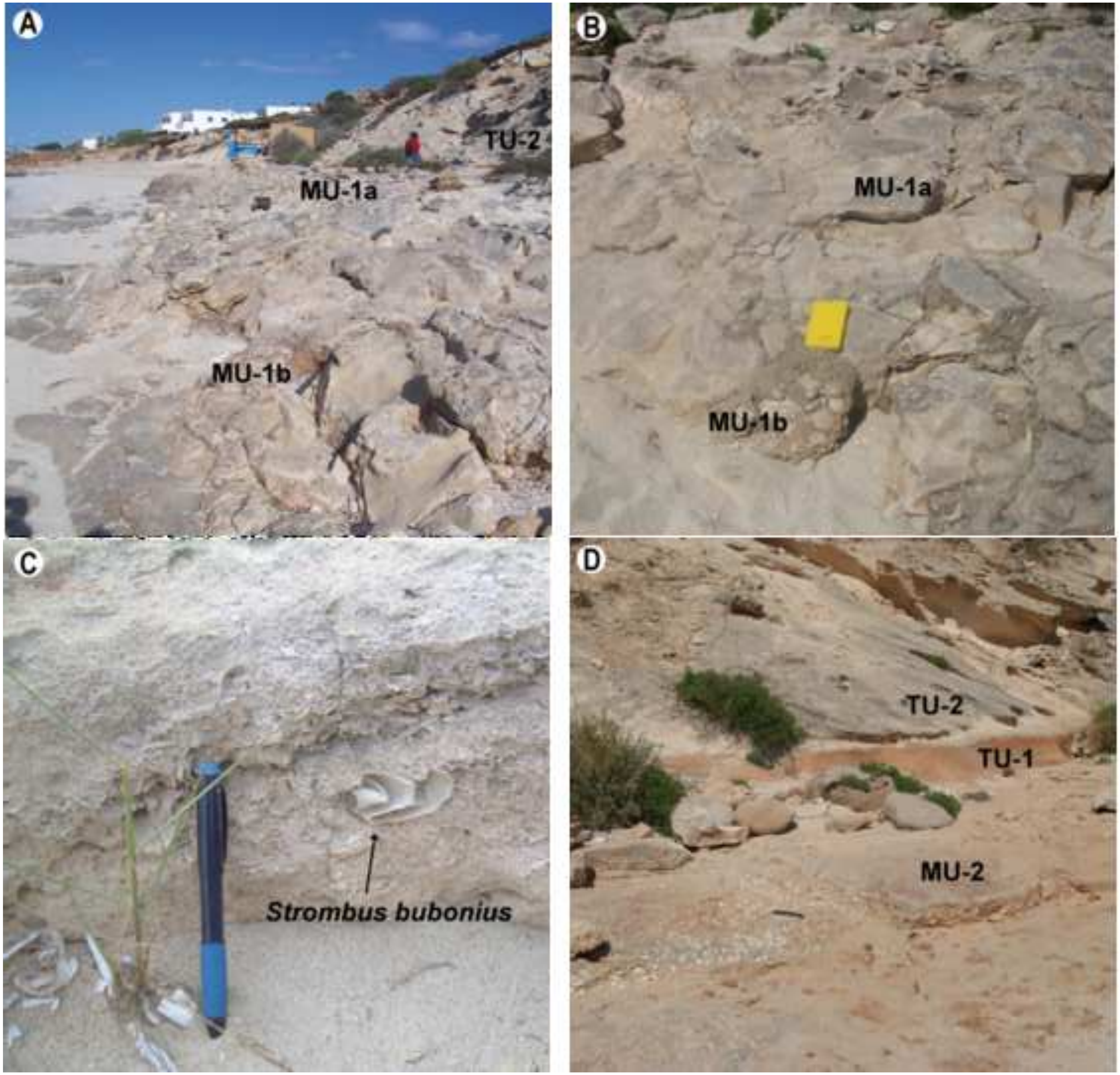

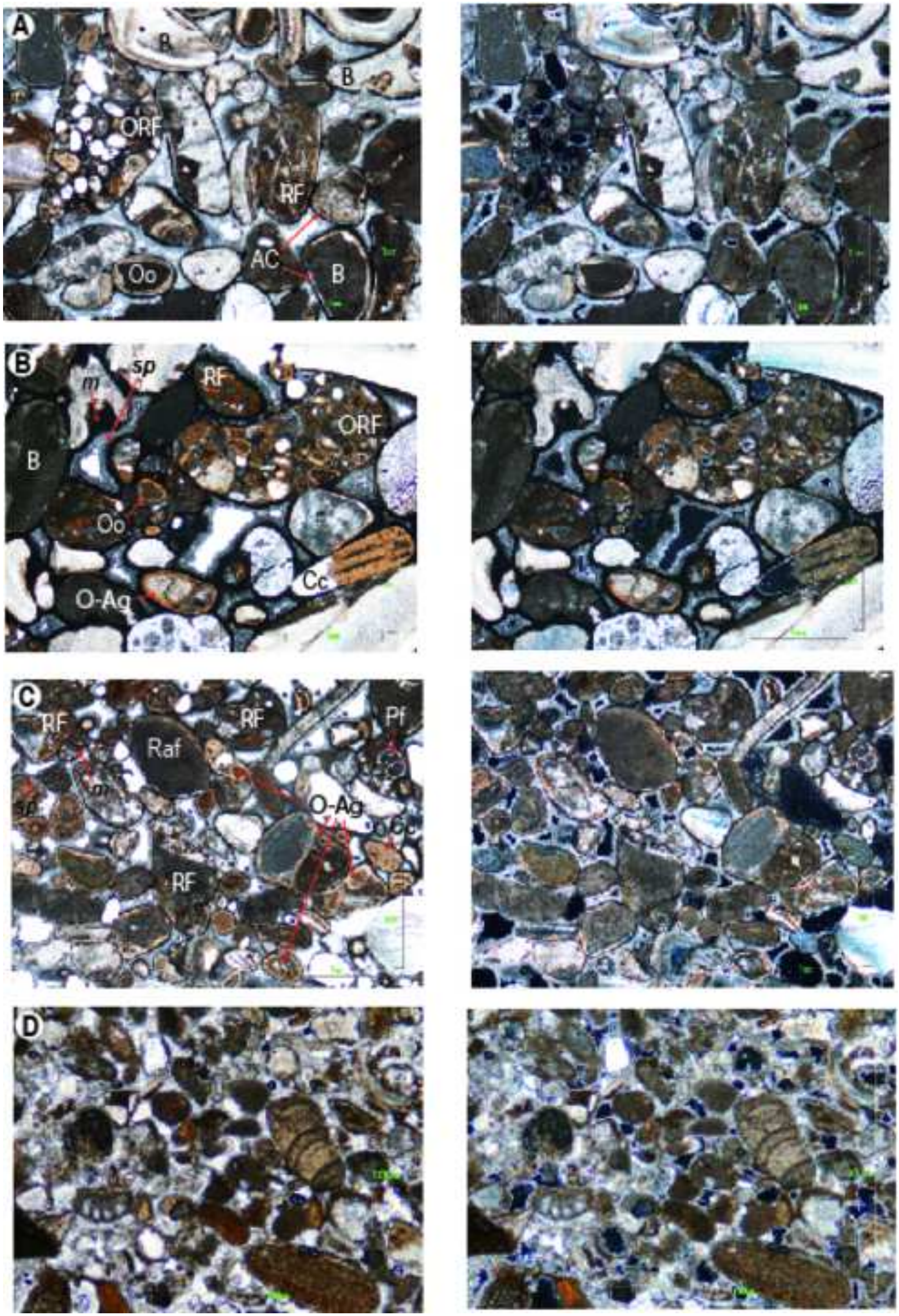
A
B
B
ORF
RF
AC
Oo
B
B
m
sp
RF
ORF
B
Oo
O-Ag
Cc
C
RF
RF
Pf
Raf
m
sp
O-Ag
Cc
RF
D

Figure 7 Click here to download Figure Figure 7.jpg

Figure 8

Click here to download Figure Figure 8.png

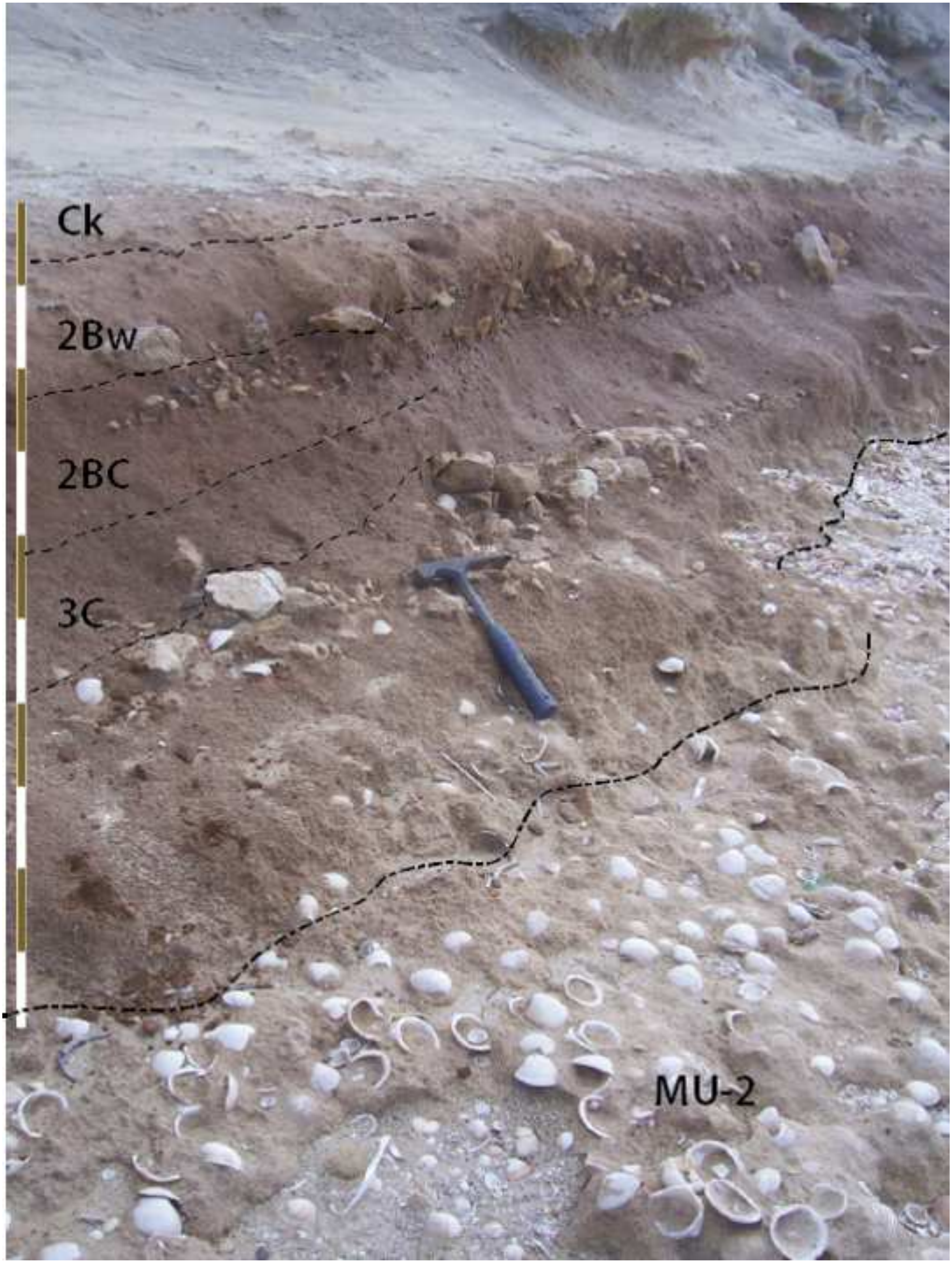

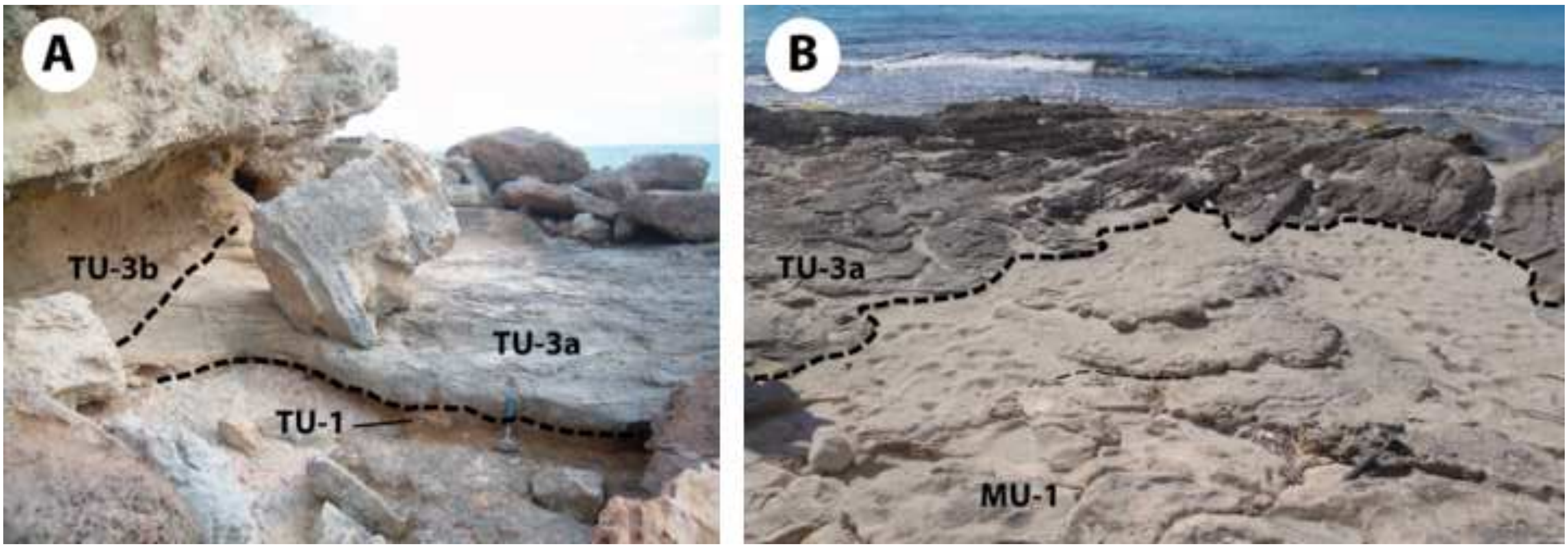
A
TU-3b
TU-3a
TU-1
B
TU-3a
MU-1

Figure 10

Click here to download Figure Figure 10.png

Figure 11 Click here to download Figure Figure 11.png

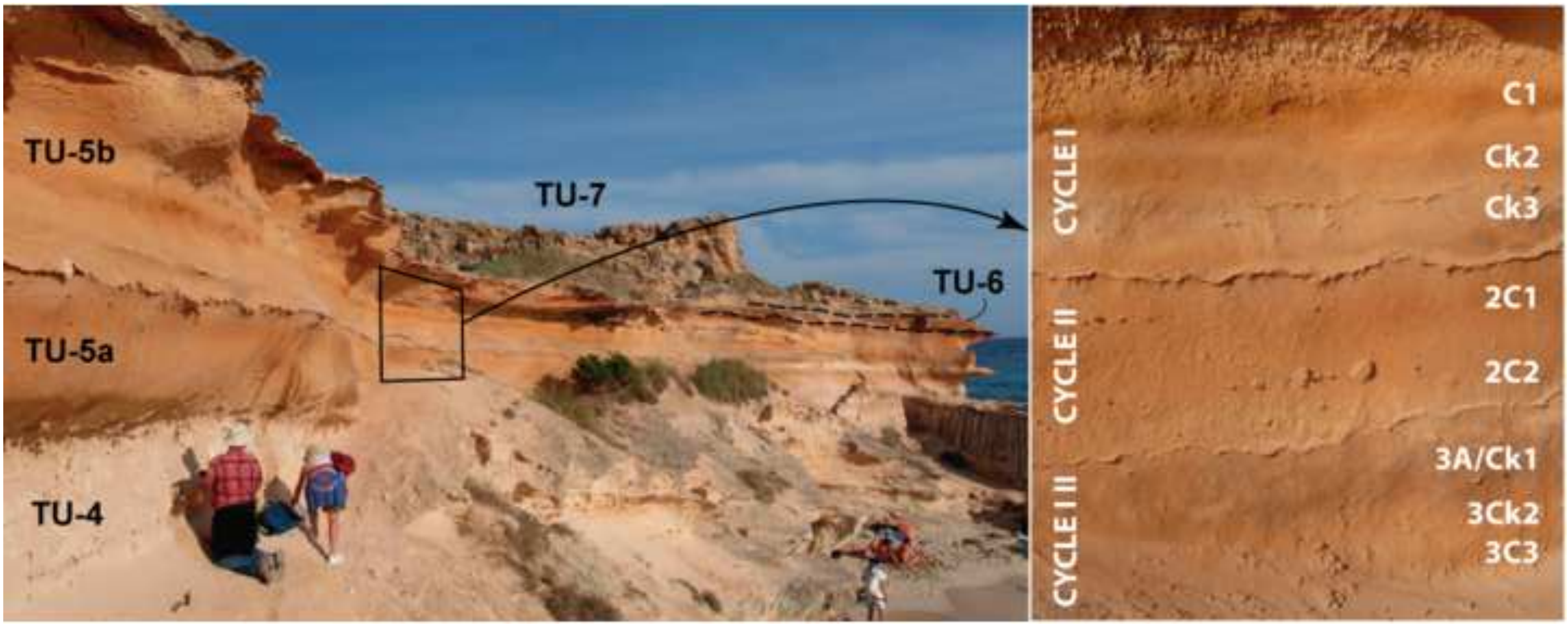

Figure 12 Click here to download Figure Figure 12.png

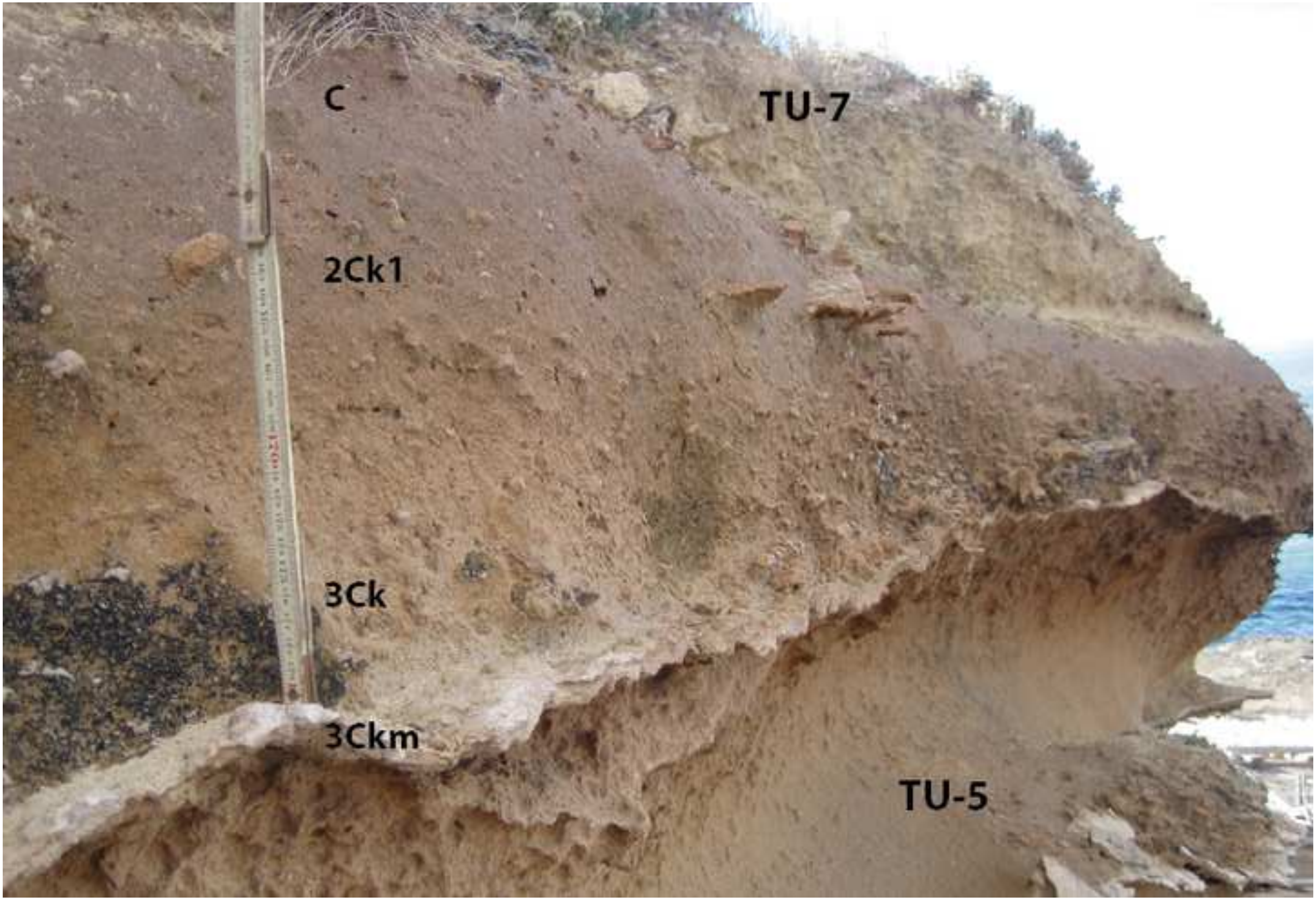

Figure 13

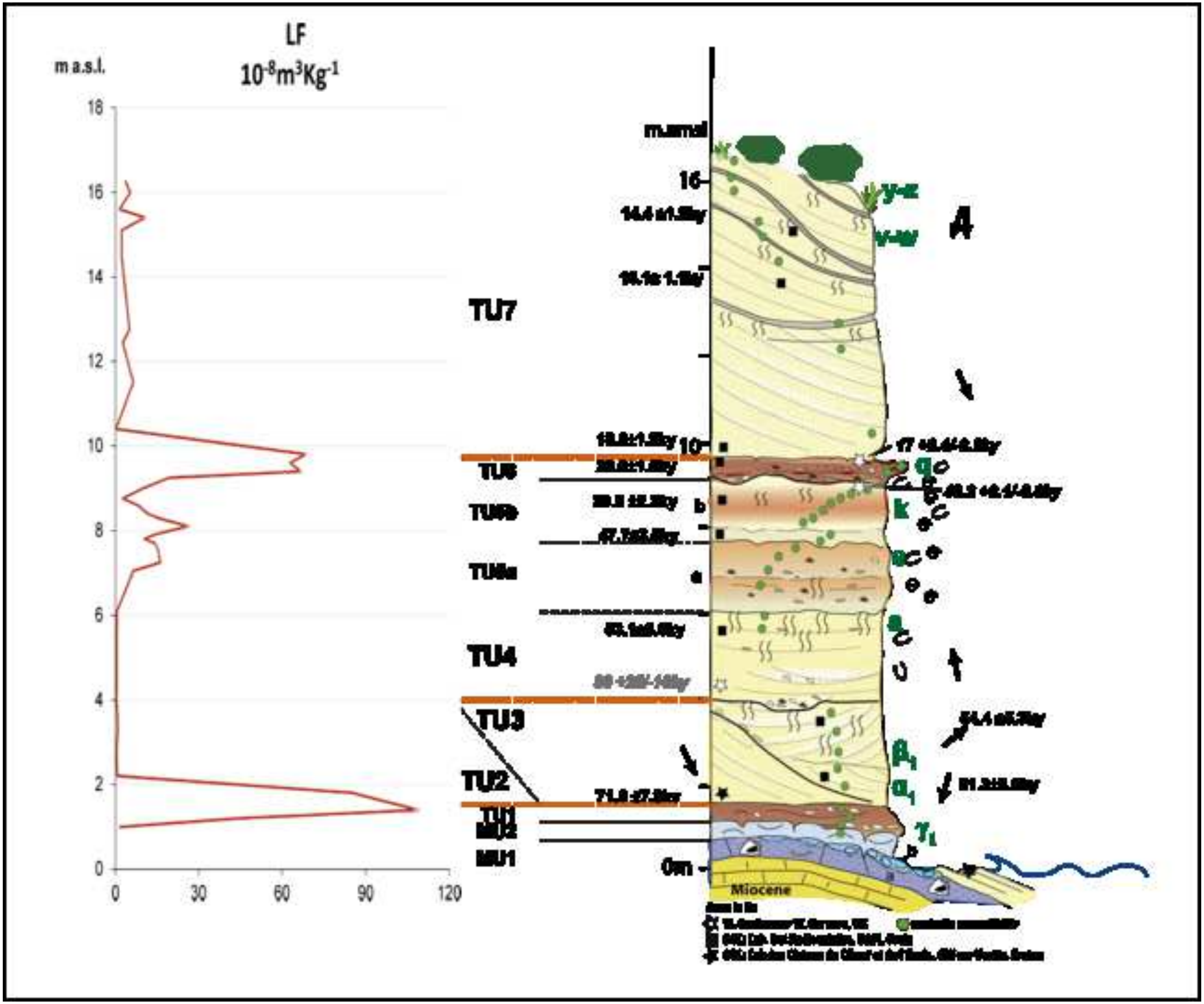
LF
10-8m3Kg-1
m a.s.l.
18
16
14
12
10
8
6
4
2
0
0
30
60
90
120
TU7
TU6
TU5b
TU5a
TU4
TU3
TU2
TU1
MU2
MU1
m.amsl
16
10
0m
A
Miocene

Figure 14

Click here to download Figure Figure 14.jpg

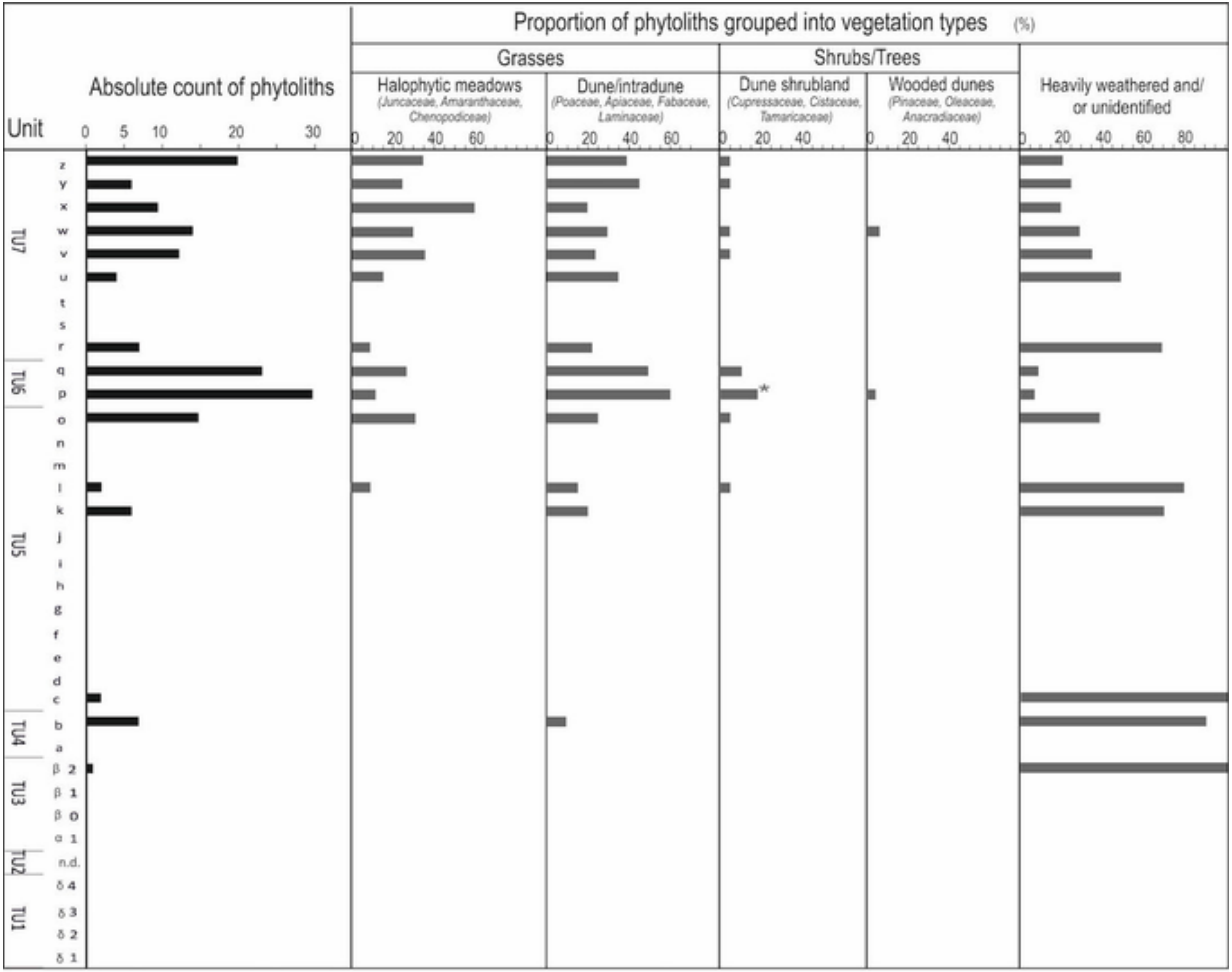

Figure 15 Click here to download Figure Figure 15.png

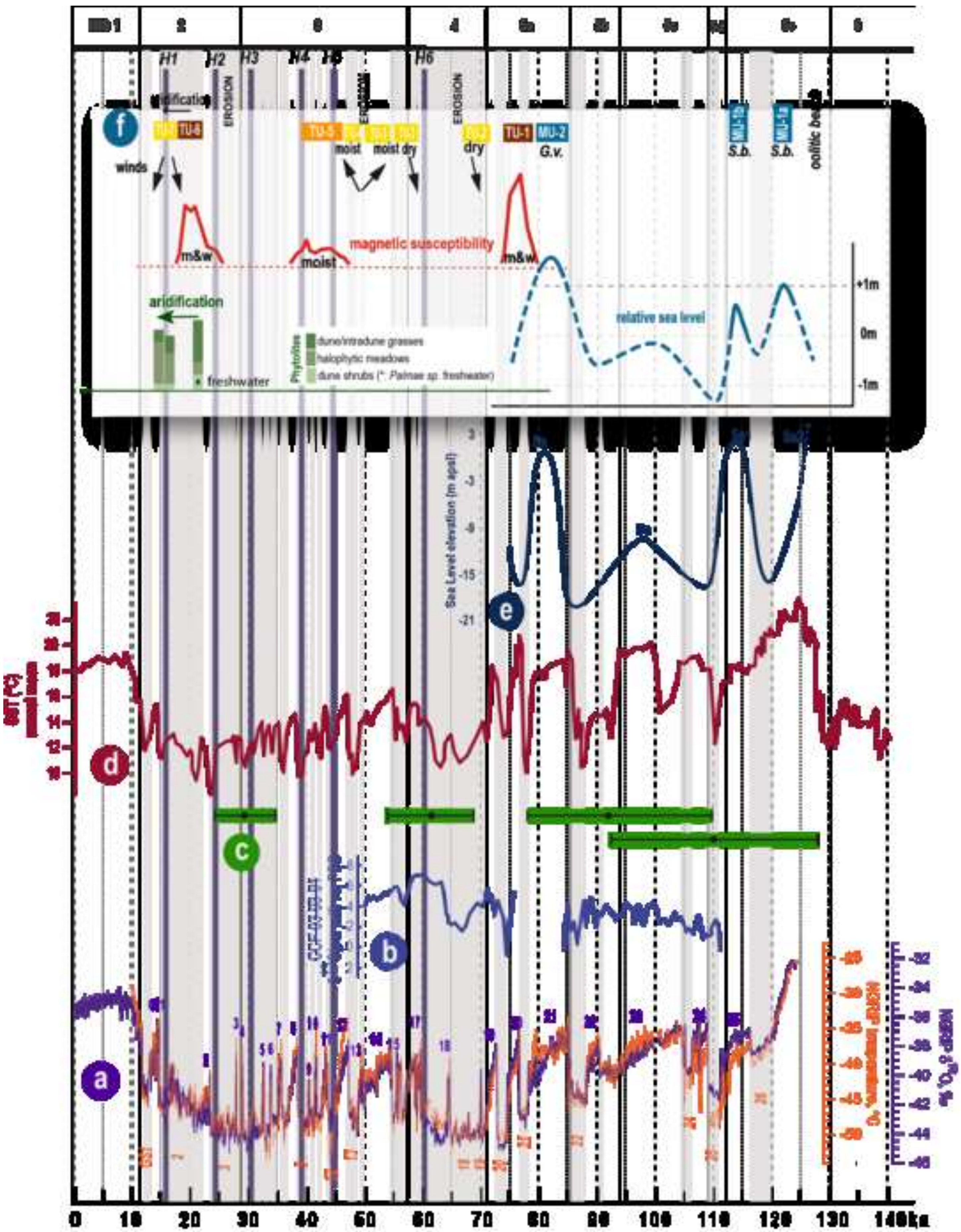

Sedimentary Unit		Horizon	depth (cm)	colour (Munsell)[1]	O.M. (%)	$CaCO_3$ (%)	Particle Size U.S.D.A. (%)				Texture Class[2]
							Coarse sand	Fine sand	Silt	Clay	
							2-0.2 mm	0.2-0.05 mm	0.05-0.002 mm	< 0.002 mm	
Terrestrial Unit 1		Ck	0-8		0.25	53	65.40	8.2	15.20	11.20	ls
Terrestrial Unit 1		2Bw	8-23	5YR 5/4 m	0.41	51	42.40	10.8	29.00	17.80	ls
Terrestrial Unit 1		2BC	23-42	2.5YR 4/4 d	0.65	48	36.50	13.30	29.70	20.50	lcs
Terrestrial Unit 1		3C	42-59	5YR 4/6 m	0.45	44	63.80	7.50	19.20	9.50	ls
Terrestrial Unit 5	Cycle I	C1	0-30	7.5YR 6/4 d	0.29	50	38.20	14.90	31.10	15.80	ls
Terrestrial Unit 5	Cycle I	Ck2	30-56	7.5YR 6/4 d	0.47	82	54.10	14.70	21.00	10.20	ls
Terrestrial Unit 5	Cycle I	Ck3	56-70	10YR 6/4 d	0.59	80	67.80	12.60	14.60	5.00	sl
Terrestrial Unit 5	C. II	2C1	0-20	10YR 6/3 d	0.5	41	81.40	6.00	7.20	5.40	sl
Terrestrial Unit 5	C. II	2C2	20-67	10YR 6/3 d	0.58	48	75.70	8.40	10.70	5.20	sl
Terrestrial Unit 5	Cycle III	3A/Ck1	0-20	7.5YR 6/6 d	0.67	81	67.00	14.30	12.10	6.60	sl
Terrestrial Unit 5	Cycle III	3Ck2	20-50	7.5YR 7/4 d	0.47	85	69.30	17.30	8.80	4.60	s
Terrestrial Unit 5	Cycle III	3Ck3	>50	10YR 7/4 d	0.38	49	82.80	8.80	5.20	3.20	s
Terrestr. Unit 6		C	0-18	7.5YR 5/4 m	0.62	52	54.10	14.30	19.30	12.30	ls
Terrestr. Unit 6		2Ck1	18-25	7.5YR 5/4 m	0.64	75	57.90	13.20	18.60	10.30	ls
Terrestr. Unit 6		3Ck2	25-42	7.5YR 6/4 m	0.72	86	60.50	16.70	15.50	7.30	ls

1. M: moist; d: dry
2. l: loam; s: sand; c: clay

Sedimentary Unit	Sample site	Mineralogy (%)								
		Magnesian calcite	Calcite	Aragonite	Dolomite	Quartz	Micas	Albite	Amorphous	Total
TU-7	z	44.3	–	31.5	12	10.6	–	–	1.6	100.00
	y	31.2	30.3	20.5	14.4	2.7	–	–	1	100.10
	x	52.2	24.3	12.4	5.3	4.1	–	–	1.8	100.10
	w	36.4	35.8	16	8.9	2	–	–	1	100.10
	v	33.5	31	25.1	7.2	1.9	–	–	1.3	100.00
	u	30.6	46.1	20.8	–	1.2	–	–	1.2	99.90
	t	55.6	–	24.3	8.5	10	–	–	1.6	100.00
	s	27.5	42	19.2	8.5	1.3	–	–	1.5	100.00
	r	40.8	–	35	22.8		–	–	1.5	100.10
TU-6	q	–	55.2	11.8	5	13.1	14	–	1	100.10
	p	–	72.4	9	–	17.7	–	–	0.9	100.00
TU-5	o	–	72.5	11.3	8.9	6.5	–	–	0.9	100.10
	n	27.5	32	23.5	14.5	1.5	–	–	1.1	100.10
	m	–	62.3	19.6	9.6	7.3	–	–	1.1	99.90
	l	66.8	–	10.1	8	13.7	–	–	1.3	99.90
	k	–	66.1	–	6.3	13.7	13	–	1	100.10
	j	–	70.9	13.2	6.5	8.2	–	–	1.1	99.90
	i	–	80.1	11.4	5	2.1	–	–	1.4	100.00
	h	57.3	–	19.4	15.2	7	–	–	1.2	100.10
	g	–	65.6	13.5	16.6	2.7	–	–	1.5	99.90
	f	–	58.1	16.8	14.4	9.1	–	–	1.6	100.00
	e	–	75.8	12	–	4.2	–	7	1.1	100.10
	d	–	68.1	17.2	4.2	9.6	–	–	0.9	100.00
	c	–	72.8	13.8	4.5	–	8.3	–	0.6	100.00
TU-4	b	35.3	–	34.3	9.6	–	19.7	–	1	99.90
	a	50.8	–	37	8.7	2.2	–	–	1.2	99.90

Table

Click here to download Table Table III.docx

Sedimentary Unit	Sample site	Major chemical components								
		Al_2O_3	Fe_2O_3 (total)	MnO	MgO	CaO	Na_2O	K_2O	TiO_2	P_2O_5
TU-7	z	0.54	0.24	–	3.13	51.52	0.26	0.11	0.03	–
	y	0.49	0.22	–	3.17	51.91	0.28	0.12	0.03	–
	x	0.36	0.19	–	3.32	51.93	0.28	0.12	0.02	–
	w	0.7	0.31	–	3.13	49.9	0.24	0.15	0.04	–
	v	0.43	0.22	–	3.21	50.14	0.27	0.1	0.03	–
	u	0.43	0.21	–	3.47	50.59	0.27	0.06	0.03	–
	t	0.8	0.36	–	3.09	50.71	0.26	0.16	0.05	–
	s	0.48	0.22	–	3.27	49.4	0.27	0.13	0.03	–
	r	0.35	0.19	–	2.97	50.98	0.26	0.07	0.02	–
TU-6	q	3.07	1.13	–	1.93	41.34	0.27	0.72	0.19	–
	p	1.41	0.51	–	1.58	48	0.15	0.28	0.08	–
TU-5	o	1.05	0.41	–	2.16	50.31	0.5	0.22	0.05	–
	n	0.32	0.14	–	3.5	50.28	0.25	0.11	0.02	–
	m	0.85	0.33	–	2.55	50.81	0.24	0.18	0.05	–
	l	2.25	0.84	–	1.95	44.35	0.63	0.48	0.13	–
	k	2.9	1.09	–	1.81	42.1	0.4	0.62	0.17	–
	j	1.84	0.68	–	1.89	45.66	0.58	0.37	0.11	–
	i	0.82	0.32	–	2.37	49.83	0.51	0.2	0.04	–
	h	0.6	0.25	–	3.08	48.41	0.74	0.11	0.03	–
	g	0.63	0.25	–	3.19	48.2	0.5	0.16	0.04	–
	f	0.87	0.36	–	3.04	46.8	0.3	0.2	0.05	–
	e	1.09	0.41	–	2.05	46.24	0.36	0.19	0.06	–
	d	0.58	0.23	–	1.89	53.26	0.25	0.14	0.03	–
	c	0.55	0.23	–	2.24	50.71	0.26	0.12	0.03	–
TU-4	b	0.27	0.13	–	2.35	54.36	0.25	0.07	0.01	–
	a	0.26	0.13	–	2.34	53.34	0.25	0.04	0.01	–